INUVIK-TUKTOYAKTUK HIGHWAY 2013-2020 GRIZZLY BEAR DNA INVENTORY: ASSESSMENT OF RESPONSE TO HIGHWAY DEVELOPMENT

JOHN BOULANGER[1] & FAYE D'EON-EGGERTSON[2]

[1]INTEGRATED ECOLOGICAL RESEARCH, NELSON, BC

[2] ENVIRONMENT AND CLIMATE CHANGE, GOVERNMENT OF THE NORTHWEST TERRITORIES

2024

MANUSCRIPT NUMBER 320

ABSTRACT

This report summarizes field collection and analyses for a grizzly bear (*Ursus arctos*) DNA mark-recapture study conducted as part of the Wildlife Effects Monitoring Program for the Inuvik to Tuktoyaktuk Highway. The main objective of this project was to assess impacts of the Inuvik to Tuktoyaktuk Highway on grizzly bears using DNA mark-recapture data collected prior to building of the highway (2013 and 2014) and after implementation of the highway (2019 and 2020). A sampling grid of 101 stations over 10,100 km^2 was used. Spatially explicit capture recapture models were used to estimate density in the grid area as well as sub-areas of the grid where bear density was likely to be affected by the highway (based upon male and female bear home range areas). Density surface models were then applied that modeled variation in density based upon landcover, historic mortality, and potential road effects. In addition, open mark-recapture models were used to assess demographic trends (apparent survival and rates of new bears in the population). 171 unique bears (76 male, 95 female) were identified over all four years of the study. Overall, a relatively even number of bears were detected in each year of the survey. Male and female bears were analyzed separately for each analysis, given likely differences in detection, as well as in movements and response to development. Female densities were relatively even throughout the duration of the study with no detected impact of the road or historic mortality using density surface models or open model methods. In contrast, male densities declined over the entire study area at a rate of approximate 5% per year. The combined male and female density estimates for the pre- and post-road periods were 9.6 (CI=8.94-10.28) and 8.55 (CI=7.69-9.17) bears per 1,000 km^2. Comparison of bear densities near the highway pre- and post-construction did not result in any apparent effects of the road. Density surface analyses did suggest a gradient of lowered density near the road, however, this gradient existed prior to road development. Bear densities in the control area of this study (16.2 and 14.4 bears/1,000 km^2) were very high compared with other barren ground grizzly bear density studies. A weak association of historic mortality in the past three years was found with male density and it is likely that harvest levels may be contributing to the lowered male apparent survival rates. Limitations of this study are the relatively short time interval between sampling (2019 and 2020) and implementation of the road, which opened in late 2017.

TABLE OF CONTENTS

LIST OF FIGURES

LIST OF PHOTOS

LIST OF TABLES

INTRODUCTION

Grizzly bears (*Ursus arctos*) are a high-profile species of local, national and international interest. Grizzly bears are an important furbearer species in the Inuvialuit Settlement Region (ISR) and have been managed under a quota since the late 1980s. As identified in the *Inuvialuit Final Agreement*, Inuvialuit have exclusive rights to hunt grizzly bears in the ISR. Grizzly bears are listed as *Special Concern* under the federal *Species at Risk Act* (COSEWIC 2012, Species at Risk Public Registry 2018). In the Northwest Territories (NWT), grizzly bears are ranked as *Sensitive* by the General Status Ranking Program and were assessed as *Special Concern* by the NWT Species at Risk Committee(SARC 2017). The NWT Conference of Management Authorities decided to not list grizzly bears under the *Species at Risk (NWT) Act* . The inclusion of grizzly bears in the Wildlife Effects Monitoring Program (WEMP) for the construction of the Inuvik-Tuktoyaktuk Highway (ITH) is based on their importance and status, their low tolerance to human disturbance, and local concern over how the proposed highway may result in changes in distribution and increased mortality of the species.

Industrial development presents several threats to bear populations including the potential for increased destruction of 'problem' bears, potential for collisions with vehicles, and the alteration and fragmentation of habitat. The highway may increase ease of access and possibly cause increased mortality resulting from hunting. However, hunting is managed under a quota system and all human-caused mortalities are counted under the quota. Any increases in mortalities due to human-bear conflicts or collisions will cause a decrease in tags available to harvesters.

Developments within the Arctic may present a relatively high risk to grizzly bear populations due to the natural low density of bears in these areas at the northern extent of their range, the relative scarcity of high-quality habitat and corresponding large area requirements, and the increased vulnerability of bears in open tundra habitats (Ross 2002). During and after construction, grizzly bears may use areas along the highway less than expected as a result of noise from construction activity, camps, and vehicle traffic. Alternatively, grizzly bears may be attracted to camps, cabins, or construction activity if waste and odours are not properly managed; these individuals may be removed from the local population as problem wildlife. After the highway is opened, additional mortalities may occur if grizzly bears that are attracted to kill sites near roads are themselves hunted. Direct grizzly bear mortality associated with vehicle collisions is expected to be a rare event.

As part of the WEMP, grizzly bear abundance monitoring in the ITH area was initiated in 2013 during the preconstruction phase of the highway, using a study design that employed hair-snagging for DNA analysis (Boulanger and Branigan 2020). There are many challenges to monitoring the effects of the road on grizzly bears given the large extent of their movements relative to the road area. The planned approach for monitoring grizzly bears was to estimate bear abundance prior to road construction, during road construction, and during regular use once constructed. Open mark-recapture methods are used to analyze the bear hair-snag DNA data over time. This allows for demographic estimates and will help to infer mechanisms for population change in the study area. The study area was designed to be large enough to allow for a "control" area and an "impact" area. Spatially explicit mark-recapture methods were used to estimate changes in bear density relative to the road area over the course of monitoring.

The objectives of the grizzly bear DNA inventory were to:

- Estimate the abundance and density of bears in the focal study area prior to (2013 and 2014) and after (2019 and 2020) implementation of the highway.
- Using baseline density surface models, assess if density relative to the road changed after implementation of the road.
- Assess if grizzly bear densities changed in the overall study area compared to areas in the focal study area that were nearer to the road.
- If possible, estimate the demography (apparent survival and recruitment) of bears in the focal study area in comparison to areas potentially affected by the road.

METHODS

Field Methods

The field design for the grizzly bear DNA study was based on studies conducted elsewhere in the Arctic, including Kugluktuk, Nunavut (Dumond et al. 2015); Hope Bay, Nunavut (C. Kent, Rescan, unpublished data); Lac de Gras, NWT (B. Milakovic, Rescan, unpublished data); and Izok Lake, Nunavut (K. Poole, Aurora Wildlife Research, unpublished data), which were developed from research initiated in British Columbia (Woods et al. 1999, Boulanger et al. 2002, Proctor et al. 2010).

The initial study area consisted of 100 grizzly bear hair-snagging tripods set out in 10x10 km grids within a 10,000 km^2 study area, which buffered the proposed highway alignment by 30-40 km, and included Richards Island and the northern portion of the Mackenzie Delta; this western area served as a spatial "control" where it was assumed that bear demographics would not be affected by the road. In 2013, part of the northwestern section of the study area was too wet for tripod deployment, resulting in the removal of seven cells, leaving 93 10x10 km cells within a 9,300 km^2 study area (Figure 1). An additional eight cells were added in 2014 to better buffer the highway and to reduce edge effects, resulting in a study area of 10,100 km^2. This design was also employed in 2019 and 2020.

Previous studies using similar methods to study barren-ground grizzly bear populations achieved adequate detection rates using 10x10 km cell size (Boulanger 2013, Dumond et al. 2015). In addition, the 10x10 km cell size (100 km^2) is smaller than the smallest annual home range of a female with cubs ($\bar{x}$ =294 km^2) determined from an earlier grizzly bear study in the Mackenzie Delta (Edwards 2009).

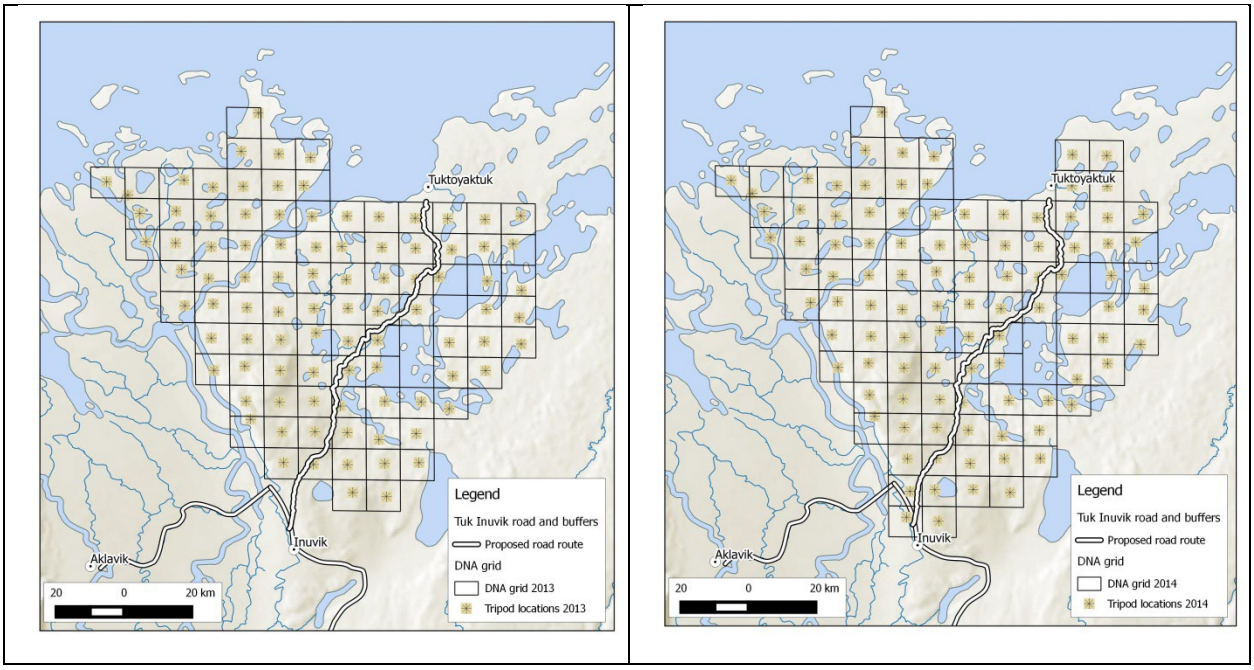

Figure 25. ITH grizzly bear DNA sampling grid, June to August 2013 and 2014. The 2014 study area was also used in 2019 and 2020.

In each year of the study, tripods were deployed for four sessions of approximately 14 days each. Tripod design consisted of six 2”x4” pieces of lumber 5’3” in length and secured at the corners with aircraft cable. Each upright 2”x 4” leg was wrapped with double-stranded 15 1/2 gauge four-point high-tensile barbed wire to trap grizzly bear hair (Photo 1). Tripod materials were prepared prior to deployment (drilling holes, wrapping barbed wire, cutting aircraft cable, etc.) and assembled in the field by teams of two using an A-Star helicopter for transportation. Tripods were deployed near or within 1-2 km of each grid cell centre in the best apparent grizzly bear habitat available – sparsely vegetated or shrubby areas adjacent to water (Edwards 2009) – although large water bodies or avoidance of cabins occasionally resulted in placement slightly further from the cell centre. Tripod bases were not anchored because large rocks are extremely uncommon on the landscape.

Photo 1. Grizzly bear hair-snagging tripod.

Lures were spread or poured atop the tripod on a piece of felt underlain by moss for absorption, and on a pile of moss and other vegetation in the centre of the tripod. Sites were revisited four times at approximately 14-day intervals to collect hair and re-bait with different combinations of blood, fish oil, and trapping lures. At the end of each session, hair samples were removed with forceps, placed in coin envelopes, and labeled with tripod number, session number, leg number, and cluster and barb number (an alpha-numeric combination) to facilitate subsampling at the lab. A propane torch was used to remove any remaining hair. Hair samples were dried each night and stored cool and dry.

All samples were sent to Wildlife Genetics International (WGI; Nelson, BC) for microsatellite genotyping. Individuals were identified using seven genetic markers, including six microsatellites and a gender marker. In 2014, an additional marker was added due to low observed heterozygosity. WGI analyzed one sample per leg, except when there were multiple clusters on a given leg, in which case up to two samples were analyzed per leg. In addition, up to two samples were analyzed from the ground per site, for a total of up to eight analyzed samples per cell/check combination. A quality threshold of a minimum of two guard hair roots or 20 underfur hairs were used. The genotyping procedures are described further in published studies from WGI (Paetkau 2003, Paetkau 2004, Paetkau et al. 2004).

Overall Analysis Approach

We use a variety of metrics to assess the impact of the road on grizzly bears based upon sampling before and after implementation of the road using a partial before and after controlled impact design (Underwood 1997) (Table 1).

Table 21. Summary of metrics used to monitor bear populations on the DNA sampling grid.

Metric	Method	Assessment of Impact
Density	SECR estimates of road vs control areas for male and female bears.	Trend in density over time for the focal study area, road area, and areas potentially affected by the road are compared pre and post implementation of the road.
Distribution and density	Distribution of bears relative to the road is modeled using density surface modeling.	Models that assume change in density as a function of distance from road are evaluated. The relative support of these models, and if they interact with implementation of the road, provides an assessment of impact of the road.
Apparent survival	Pradel open model estimates apparent survival (deaths and/or emigration) for male and female bears on grid and covariates.	The estimate of apparent survival estimates the fidelity and survival of bears on the sampling grid. These are compared to estimates from sub regions near the road based on estimated bear home range locations.
Rates of addition	Pradel open model estimates rates of addition (births and/or immigration) for male and female bears on grid and covariates.	The estimate of rates of addition can help assess if there is a greater influx of new bears on the grid over time as well as the relative influence of additions versus survival on overall trend. If the road has an impact, then it is hypothesized that rates of addition will be lower for bears near the road.

Spatially Explicit Mark Recapture Analysis

Spatially explicit capture-recapture (SECR) methods (Efford 2004, Efford et al. 2004, Efford et al. 2009, Efford 2011), also known as spatially explicit mark-recapture methods, were used to estimate grizzly bear density. Spatially explicit methods estimate the spatial scale of movements for bears that are detected repeatedly during sampling to estimate the area that these individual bears covered. Unlike closed models, which pooled data from multiple tripods within each session for each bear, the SECR method used multiple detections of bears at unique tripods within a session to model bear movements and detection probabilities. Using this information, the detection probabilities of grizzly bears at their home range center (g_0), the spatial scale of grizzly bear movements around the home range center (σ), and bear density (D) were estimated. An assumption of this method is that grizzly bear home range can be approximated by a circular symmetrical distribution of use (Efford 2004). The actual shape and configuration of the sampling grid was used in the process of estimating home range, scale of movements and density, therefore accounting for the effect of study-area size and configuration on the degree of closure violation and subsequent density estimates. For the study area, a habitat mask that accounted for areas unusable to grizzlies (such as the ocean and large lakes within and in the immediate area of the sampling grid) was used to ensure the study area size included only useable habitat.

Analyses were conducted separately for each sex with years treated as sessions. This approach was optimal given that male and female bears have different scale of movement and detection SECR parameters as well as likely differences in distributions across the study area (Boulanger et al. 2014). By treating the years as sessions, it was possible to test for differences in densities between years as well as test for differences in distribution in the context of density surface modeling.

As an initial step in the modeling process, the effective sampling area (termed the habitat mask) of the grid was estimated. The effective sampling area in the context of spatially explicit modeling is the grid and surrounding area where a bear had a non-zero probability of detection. This area extends beyond grid boundaries given that bears can travel into the grid during sampling. Using an iterative process this was estimated to be the grid and a buffer area of 30 km surrounding the grid. Significant water bodies such as the ocean and large lakes were also modeled as non-habitat and density was set to 0 in these areas as indicated by no mask centroids over these areas (Figure 2). This mask area was used for both the male and female analyses.

Base Detection Model Analysis

A first step in the analysis was modeling the detection and redetection of male and female bears at the tripod sites. For this analysis, yearly differences in detection parameters (g0) and spatial scale (σ) were modeled. In addition, potential behavioural effects of sampling such as change in detection of individual bears after initial detection were considered. In detail, models that changed detection if the bear was detected in the preceding session (termed *B*) or detected in any previous session (b) were considered. In addition, we considered models that assumed a site-specific behaviour response (termed *bk*) where bears are more or less likely to visit a site after it has been previously visited.

The relative fit of base detection models, as well as density surface models, was evaluated using the sample size adjusted Akaike Information Criterion (AIC_c). The model with the lowest AIC_c score was considered the most parsimonious, thus minimizing estimate bias and optimizing precision (Burnham and Anderson 1998). The difference in AIC_c values between the most supported model and other models (ΔAIC_c) was also used to evaluate the fit of models when their AIC_c scores were close. In general, any model with a ΔAIC_c score of less than two was worthy of consideration.

Density Surface Modeling

Structural Relationships Between Habitat Covariates Using Density Surface Modeling

Spatially explicit mark-recapture models were used to model variation in bear density on the study grid area and to estimate population size and density for areas that were in the proximity of the ITH. This approach also provided a baseline model of density in the study area to allow testing of road effects.

Spatially explicit mark-recapture methods estimate density for a systematic grid of points/centroids that are overlaid on the study area (termed the habitat mask; Figure 2). For non-spatial models it is assumed that bear density is equal for each mask point. Density surface models estimated bear density at each mask centroid based upon habitat covariates summarized around the mask point. The fit of each of the density surface models was then

compared to models that assumed similar density for each mask point. This approach is similar to resource selection function (RSF) models that are fit to detection frequencies at DNA collection sites with the strong advantage that the response surface is a systematic grid of points rather than trap locations (Efford and Dawson 2012, Efford and Fewster 2013, Royle et al. 2013, Royle et al. 2014, Boulanger et al. 2018).

"Activity centers" of bears were estimated using baseline SECR models (Royle et al. 2013, Royle et al. 2014, Kendall et al. 2015). This approach provides an initial assessment of likely locations of home range centers of bears, however, it is also influenced by trap placement and edge areas of the grid (Efford 2014a). Therefore, density surface models were used to further model and explore factors associated with observed bear density on the sampling grid (Boulanger et al. 2018).

Density surface model estimates are based on estimated locations of bear home range centers. Habitat was summarized based on the SECR scale parameter value (σ) for males and females (11.1 and 8.1 km) from the base SECR analysis detailed later in the report. Using these values accounted for the differing scale of home range selection of males and females while still maintaining larger-scale independence of SECR mask points.

Remote sensing data and previous RSF analyses based upon collared grizzly bears were used (Edwards 2009) to formulate density surface models. The covariates used for density surface modeling included RSF scores, which categorized each 28.5 m^2 patch of vegetation, from Edwards (2009) as well as habitat covariates used to formulate the RSF models (Table 2). The coverage of the RSF and landcover surfaces included all tripod sites but excluded some of the areas in the southwest of the sampling grid (Figure 2); scores for these areas were based upon scores of the closest mask centroid. Coverage of the RSF model extended to where the hair collection sites occurred and therefore the overall effect of missing RSF scores for peripheral areas probably was not substantial. Dwarf shrub and water were the most dominant landcover forms in the study area comprising over 50% of centroid buffer areas (Table 2, Figure 2).

Table 22. Habitat covariates used for density surface modeling based upon Edwards (2009). The mean, min, and max percentage area in a 1 km buffer area around each centroid is also given.

Habitat Covariate	Dominant Land Cover Features	Mean	Minimum	Maximum
Forest				
Coniferous				
Closed spruce	Closed mixed needleleaf	0.1	0.0	11.1
Open spruce	Open spruce	0.2	0.0	9.7
Deciduous				
Closed Deciduous	Closed birch	0.9	0.0	41.7
Open Deciduous	Open birch	2.2	0.0	36.0
Shrub				
Dwarf shrub	Dwarf shrub	28.3	0.0	88.6
Low shrub lowland	Low shrub willow alder	5.2	0.0	42.7
Tall shrub	Closed tall shrub	6.0	0.0	66.5
Low shrub upland	Low shrub-tussock tundra	6.0	0.0	42.7
Barren/sparse				
Sparse vegetation	Sparse	4.6	0.0	99.3
Herbaceous				
Herbaceous	Mesic dry meadow	6.1	0.0	84.3
Wet herbaceous	Wet graminoid	6.5	0.0	55.0
Water				
Water	Clear water	24.7	0.0	100.0

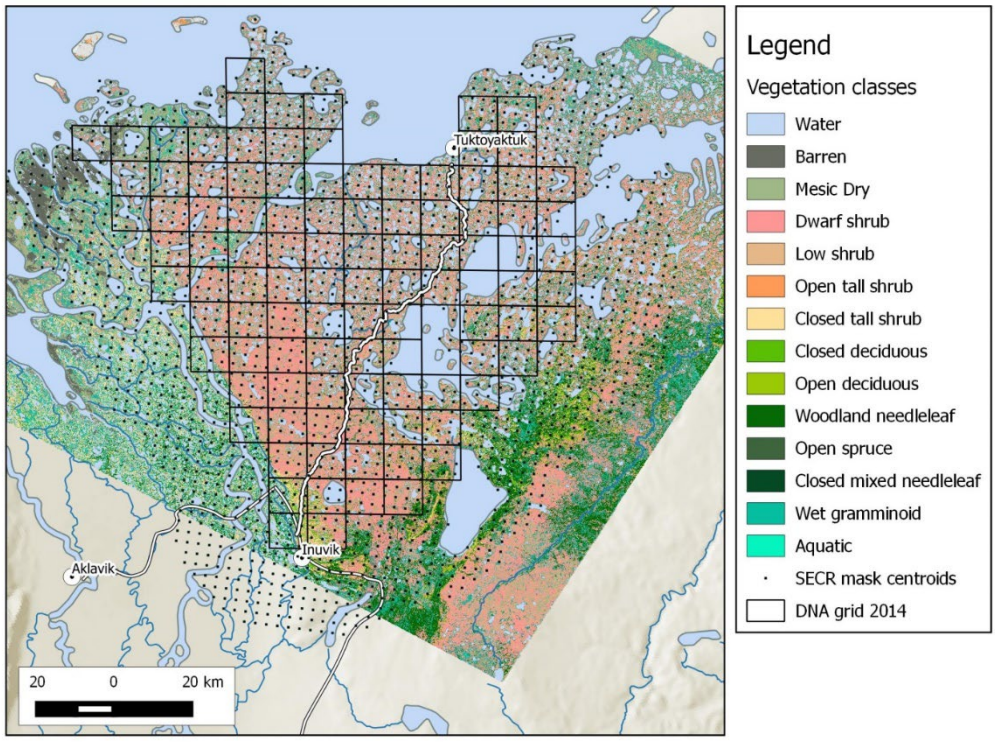

Figure 26. Habitat mask centroids, DNA tripod sites, and landcover covariates used in the density surface model exercise.

It is likely that the proportion of habitat classes across centroids were structurally related given the similarity of land cover and likely associations among different vegetative types. In order to determine the most parsimonious combinations of covariates to describe grizzly bear density, we assessed how covariates were related to each other. Principal components analysis was used to discern structural relationship between habitat covariates to allow further interpretation of density surface modeling results (Tabachnick and Fidell 1996, McGarigal et al. 2000). The results of this analysis are given in Appendix 2.

Effect of Yearly Human-caused Mortality

An additional covariate that was considered in the density surface model was human-caused mortality of bears that occurred historically in the study area as well as during sampling. It was hypothesized that longer term spatial mortality might influence density variation on the sampling grid area with shorter term mortality creating additional variance in the distribution of home range centers. Human-caused mortality within the SECR mask area averaged 3.3 (sd=1.7, min=1, max=7) and 8.8 (sd=3.1, min=3, max=12) female and male per year from 2010-2020. The pattern of mortality was fairly even relative to the road during this time (Figure 3). If only the DNA grid area is used, then mortality was 2 (sd=0.82, min=1, max=4) and 5.6 (sd=2.5, min=2, max=10) female and male bears per year from 2010-2020.

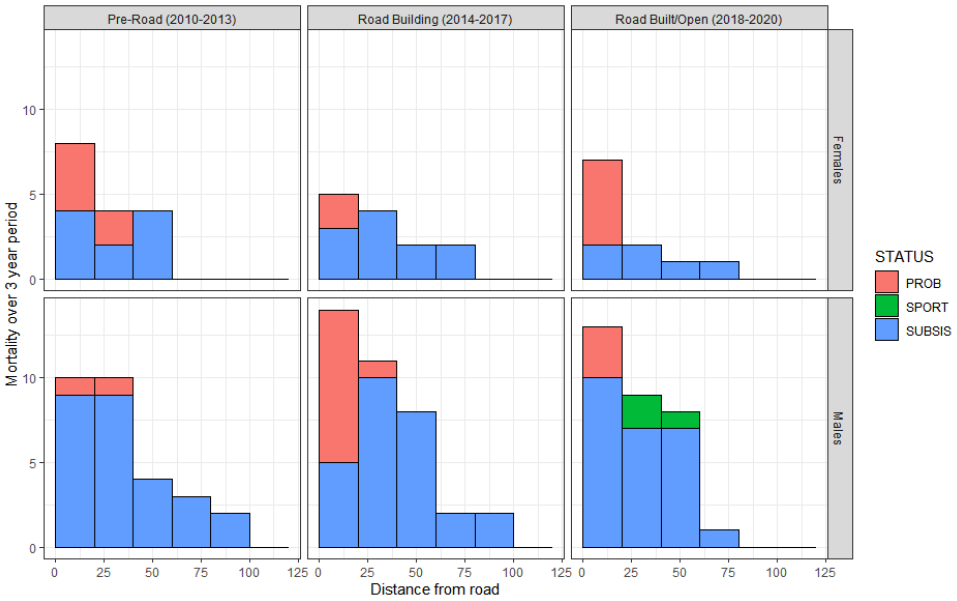

Figure 27. Mortality of bears as a function of distance from road by phase of analysis for the area defined by the SECR mask extent (Figure 2). Sub-bars denote mortality type (PROB-problem bear, SPORT-sport hunting, SUBSIS-subsistence hunting).

SECR mask covariates were derived by buffering mortality locations by home range buffers (19.9 km and 27.3 km for female and male bears). The intersection of buffered locations with mask points was then tallied to create a mortality score for each mask point. The scores for the year of sampling, the cumulative count of mortalities for the current year (*Mortsyr*) previous three years (*Morts3yr*), and previous ten years (*Morts10yr*) were then tallied to create three mortality covariates. These covariates tested the immediate and longer-term effects of human-caused mortality (three and ten years) on density and distribution. More details on mortality models are given in Appendix 3.

Estimation of Road Effects

Once a base habitat model was established, further covariates were considered to test for influence of the road on grizzly bears compared to overall demographic trends in the entire study area (Table 3). Given that sampling occurred in yearly intervals prior to the road (2013-2014) and after the road (2019-2020), it was possible that changes in density were minimal in the yearly intervals compared to the five-year interval between the 2014 and 2019 surveys. To model this, a *Period* covariate was used which tested for mean change in density between the two sampling periods. Various models of road effect were considered. The *StrataHR* covariate tested for overall difference in mean density between the home range-based road-affected areas (Figure 2) whereas the *ZOIHR* covariate assumed that density would change in a log-linear trend from distance from road=0 up to the *StrataHR* boundary (19.9 and 27.3 km for females and males) after which it would be constant. The *ZOIsigma* covariate tested for smaller scale effects based on sex-specific σ values (8.1 and 11.1 km for females and males). The spline term used generalized additive models (Hastie and Tibshirani 1990) to test for non-linear trends in density relative to the road which contrasted with the constrained zone of influence (ZOI)-based relationships. The road affect covariates were tested with and without the temporal covariates (Period and Year) to test

pre-existing relationships prior to the road (2013-2014). A supported interaction term (i.e., *Period*ZOIHR*) would suggest a change based on presence of the road.

Table 23. Temporal and road-based covariates used in density surface model analysis.

Covariate	Description
Temporal	
Year	Density varies each year sampled
Period	Density varies prior (2013-2014) and post road (2019-2020)
Road effects	
StrataHR	Density varies within and outside HR-based strata (Figure 4)
ZOIsigma	Density changes log-linearly from road up to sigma for males and females and is then constant
ZOIHR	Density changes log-linearly from road up to the boundary of the HR strata and is then constant
Spline(road)	Polynomial estimation of change in density with distance from road.

Regional Estimates of Population Size Relative to The Proposed Road

Stratified Estimates of Areas Near Road

The DNA grid area was stratified based on likely areas of movement and detection for male and female bears relative to the route of the road. For this approach, SECR centroids that were within the 19.9 or 27.3 km distance of the road were classified as male or female strata, with centroids beyond the buffers being categorized as "control" strata (Figure 4). The 19.9 or 27.3 km distances were based upon estimates of movement during sampling from SECR analysis of the 2013-2020 SECR data set. The realized or average number of grizzly bears that could potentially encounter the road at any one time was estimated by spatially explicit mark-recapture models (Efford and Fewster 2013). Estimates from models that assumed constant density throughout the study area were compared to density surface models that accounted for habitat specific variation in density for the entire grid and the road strata. Using this approach allowed specific estimates for the road buffer areas in comparison to areas outside the buffer (Stenhouse et al. 2015).

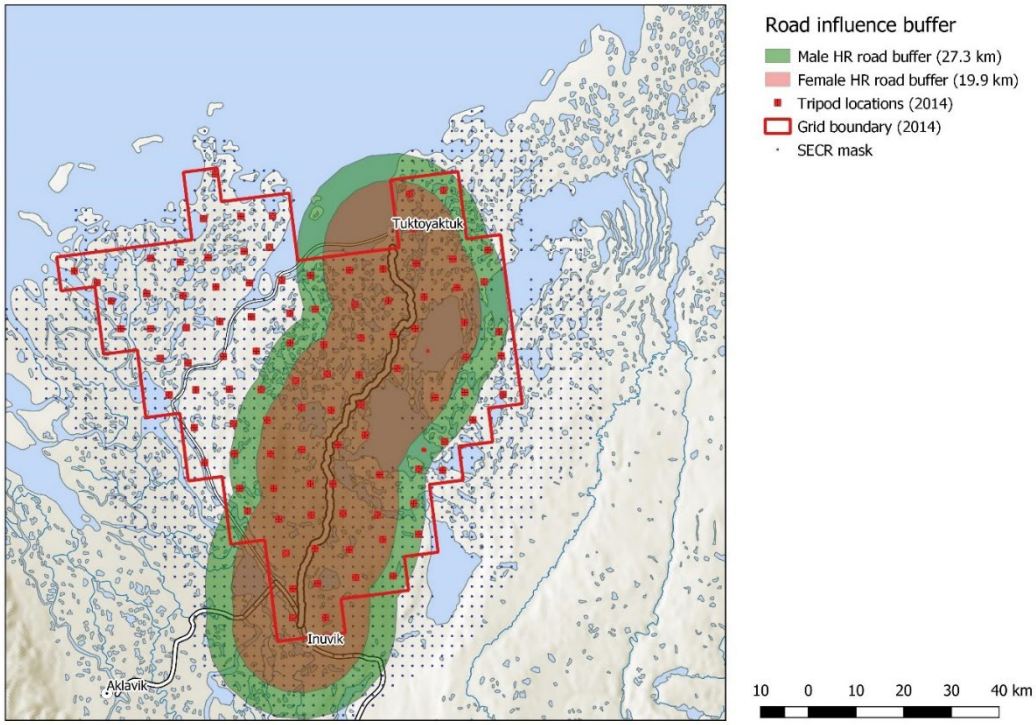

Figure 28. ITH with SECR based buffers of 19.9 km (females) and 27.3 km (males) which define the potential area of greatest influence of the road on grizzly bears during sampling. Tripod locations used for 2014, 2019, and 2020 along with the DNA grid boundaries (used for regional estimates) are delineated. In addition, centroids of the habitat mask used by the SECR model are shown.

Open Model Demographic Analyses

The Robust design (Pollock and Otto 1983) Pradel model (Pradel 1996) in the *opencr* R package (Efford 2019) was used to estimate demographic parameters from the 2013 and 2014 data. Detection probability (p*) was estimated for each year using the Huggins closed population model (Huggins 1991) and the change in population size (λ), as well as apparent survival (ϕ) and rates of additions between years (f), was estimated using the Pradel model. Apparent survival (ϕ) is the probability that a bear that was on the grid in one sampling year would still be on the grid in the next sampling year. It encompasses both deaths and emigration from the sampling grid. Rate of addition (f) is the number of bears on the grids in the current year per bear on the grid in previous year. It encompasses both births and immigration of bears from outside the grid area between sampling years. Apparent survival and rates of addition are added together to estimate change in population size (λ) for the interval between each sampling year. Population rate of change is equivalent to the population size for a given sampling period divided by the population size in the previous sampling period ($\lambda=N_{t+1}/N_t$). Given this, estimates of λ will be one with a stable population, less than one if the population is declining and greater than one if the population is increasing.

Recently, SECR-based versions of the Pradel model have been derived that allow modeling of site layout as well as estimation of movement between years of sampling (Efford et al.

2020). A secondary analysis was conducted using this approach. This analysis used the most supported models from the traditional approach with the SECR detection parameter as well as various models of between-year movement. Namely, bivariate normal and bivariate exponential sex-specific models were considered. The general approach of these models is to estimate change in home range center based on a normal or exponential distribution. Estimates of demographic parameters were then compared to the traditional closed Pradel model estimates.

Analyses were conducted primarily using the *secr* (Efford 2014b) and *opencr* (Efford 2019) package in *R* (R Development Core Team 2009). Results were plotted using the *ggplot2* (Wickham 2009) *ggmap* (Kahle and Wickham 2013), with GIS analyses conducted using the *sf* packages (Pebesma 2018) in R, as well as the QIS software program (QGIS Foundation 2020).

RESULTS

Data Summary

The number of bears detected (72-79) and number of detections (113-123) was similar for all years of the study, with no apparent change between the 2013-2014 pre-operational and 2019-2020 operational periods (Table 4). More female bears than male bears were detected in all years of the study, and they were detected at more sites.

Table 24. Summary counts of the number of grizzly bears detected during the ITH grizzly bear project by year and sex. All samples from an individual bear were pooled within each session for this summary for Detected (bears detected per session), Unmarked (new bears each session), Cumulative (cumulative count of new bears detected) and Frequencies (number of individual bears captured during one to four (all) sessions that year). Site detections include all unique bear visits to sites whereas sites visited is the number of different sites with detections per session. Totals are given for males and females combined (M+F), as well of the percentage of detections that were female bears.

Counts	Females					Males					M+F	
	1	2	3	4	Total	1	2	3	4	Total	Total	%F
2013												
Detected	11	20	22	21	74	12	13	13	11	49	123	60%
Unmarked	11	15	12	8	46	12	8	7	2	29	75	61%
Frequencies	25	15	5	1	46	16	7	5	1	29	75	
Cumulative	11	26	38	46	46	12	20	27	29	29	75	61%
Site detections	11	20	33	24	88	13	14	15	14	56	144	61%
Sites visited	10	13	21	19	63	10	11	13	12	46	90	70%
Sites available	93	93	93	93	372	93	93	93	93	372	372	
2014												
Detected	13	22	20	18	73	10	15	13	12	50	123	59%
Unmarked	13	19	6	7	45	10	11	4	7	32	77	58%
Frequencies	20	22	3	0	45	18	10	4	0	32	77	
Cumulative	13	32	38	45	45	10	21	25	32	32	77	58%
Site detections	14	25	25	20	84	13	18	14	14	59	143	59%
Sites visited	12	19	21	14	66	11	14	12	11	48	90	73%
Sites available	101	101	101	101	404	101	101	101	101	404	404	
2019												
Detected	13	35	21	9	78	6	13	9	7	35	113	69%
Unmarked	13	27	4	5	49	6	9	5	3	23	72	68%
Frequencies	26	18	4	1	49	12	10	1	0	23	72	
Cumulative	13	40	44	49	49	6	15	20	23	23	72	68%
Site detections	13	39	24	11	87	8	14	9	9	40	127	69%
Sites visited	10	25	18	11	64	8	14	9	9	40	86	74%
Sites available	101	101	101	101	404	101	101	101	101	404	404	

Counts	Females					Males					M+F	
	1	2	3	4	Total	1	2	3	4	Total	Total	%F
2020												
Detected	12	24	26	15	77	11	9	10	6	36	113	68%
Unmarked	12	17	15	3	47	11	4	4	3	22	69	68%
Frequencies	27	10	10	0	47	12	7	2	1	22	69	
Cumulative	12	29	44	47	47	11	15	19	22	22	69	68%
Site detections	14	27	30	23	94	13	14	12	7	46	140	67%
Sites visited	12	24	22	19	77	11	12	12	7	42	104	74%
Sites available	101	101	101	101	404	101	101	101	101	404	404	

Summaries of movements of males and females suggest widespread movement on the grid in all years, especially for males. The distribution of locations suggests higher numbers of bears to the northwest of the sampling area (Figure 5).

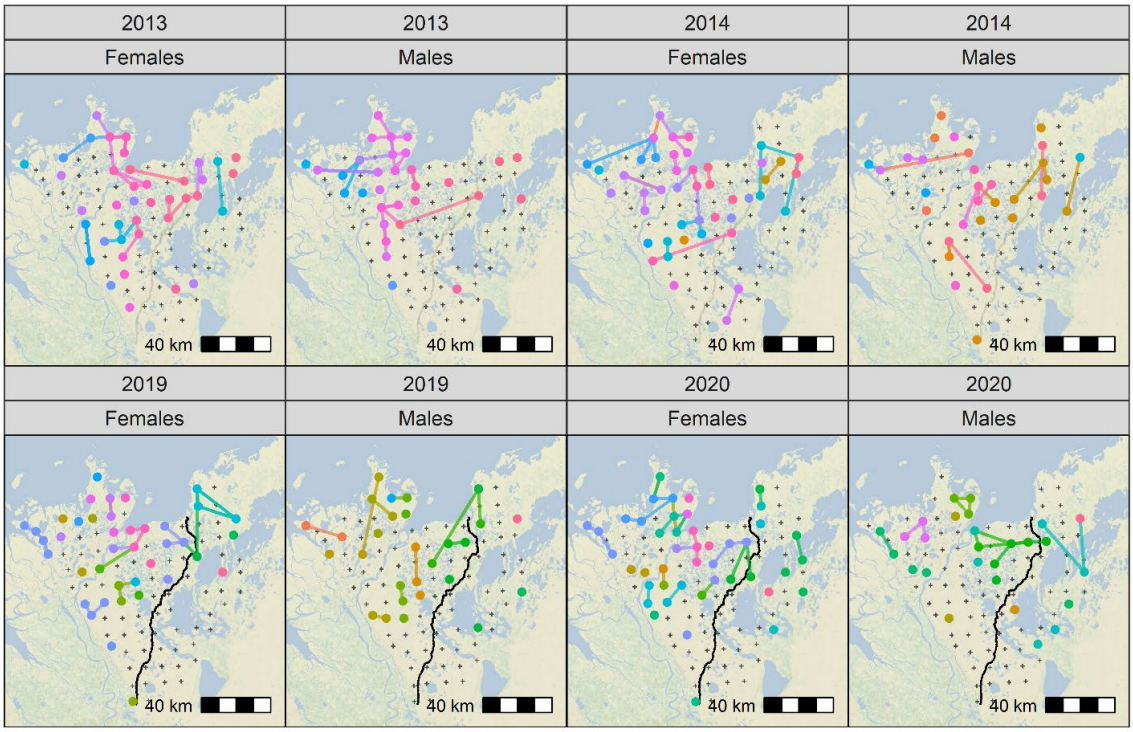

Figure 29. Bear detections for male and female bears each year. Each individual bear is noted by a unique color. Multiple detections for individual bears are linked by lines indicating approximate movement paths.

Spatially Explicit Mark-recapture Analysis

Female SECR Analyses

Spatially explicit model selection focused on variation in detection probability at home range center (g_0) and movement (sigma, σ). Models that considered behavioural change in g_0 were most supported (Table 5, Models 1-4). Models that considered change in site-specific

detection probabilities after detection (*bk*) were most supported, followed by change in individual bear detection (*b and B*) after initial detection.

Other models that were considered were year-specific variation in density, detection, and scale of movement as well as site-based covariates for detection and scale of movement. Year-specific variation in density was considered further in the context of density surface modeling discussed later.

Table 25. Female spatially explicit model selection with models indicated by assumptions made about density, detection at home range center (g_0) and scale of movement (σ). Model notation includes: b = change in detection if the bear was detected previously (in any session), B = change in behaviour of bear in previous session to detection. bk = where bears are more or less likely to visit a site after it has been previously visited, constant = single value for parameter. Sample size adjusted AIC_c, the difference in AIC_c from the most supported model (ΔAIC_c), AIC_c weight (w_i), number of model parameters (K) and log-likelihood are given.

No	Density	Detection (g_0)	Scale (σ)	AIC_c	ΔAIC_c	w_i	K	LL
1	constant	bk	constant	2583.27	0.00	0.79	4	-1287.5
2	constant	bk	year	2587.54	4.27	0.09	7	-1286.5
3	constant	bk+year	year	2588.18	4.90	0.07	10	-1283.5
4	year	bk	constant	2589.16	5.89	0.04	7	-1287.3
5	constant	bk*year	constant	2594.33	11.06	0.00	10	-1286.5
6	constant	b	constant	2617.37	34.10	0.00	4	-1304.6
7	constant	b+year	constant	2622.37	39.10	0.00	7	-1303.9
8	constant	B+year	constant	2623.15	39.88	0.00	7	-1304.3
9	year	b	constant	2623.28	40.01	0.00	7	-1304.3
10	constant	constant	constant	2626.07	42.79	0.00	3	-1310.0
11	constant	year	year	2626.91	43.63	0.00	9	-1303.9
12	year	b+year	constant	2627.63	44.35	0.00	10	-1303.2
13	constant	constant	year	2628.92	45.64	0.00	6	-1308.2
14	constant	year	constant	2631.29	48.01	0.00	6	-1309.4
15	year	year	year	2632.53	49.25	0.00	12	-1303.4
16	year	constant	year	2633.36	50.09	0.00	9	-1307.2
27	year	year	constant	2636.78	53.51	0.00	9	-1308.9

Plots of the detection function from Model 1 in Table 5 revealed an increase in detection at home range center (g_0) after initial detection (Figure 6) for a site. Estimates of g_0 were 0.09 and 0.29 at initial and subsequent detection with the spatial scale parameter (σ) of 8126.2 meters defining the scale of movement. This basically implies that once a site detected a bear it was more likely to detect bears in subsequent sessions.

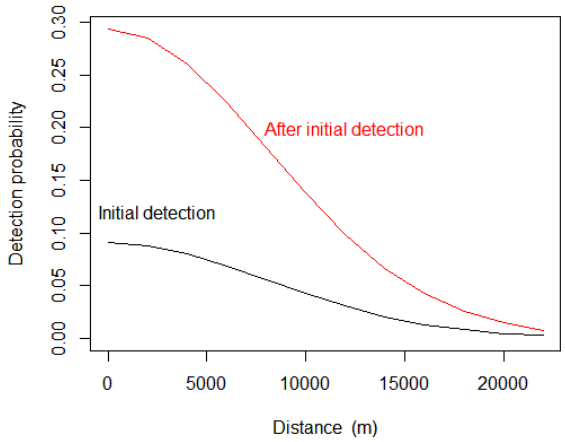

Figure 30. Spatially explicit detection function from Model 1 (sites with different initial detection and redetection rates), Table 5. The black line is the initial detection function, and the red line is the detection function after initial detection.

The base SECR model was used to estimate home range centers and associated areas. This revealed a northwest to southeast density gradient in all years of sampling with no large-scale changes in density for any of the years of sampling (Figure 7). This analysis also estimates the relative density of bears in the area based on estimated home range centers for marked and unmarked bears. This analysis is sensitive to trap placement and therefore the density surface models presented next are a better representation of actual density.

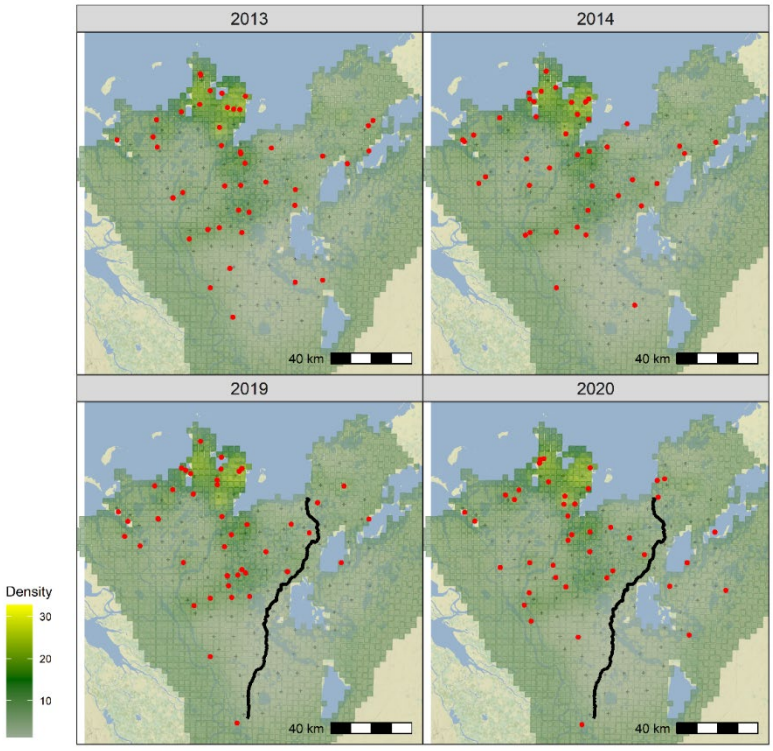

Figure 31. Estimated home range centers for each year of the study for female bears. The most supported base SECR model was used to generate estimates. Relative density based on home range centers is also depicted.

Variation in Density on The Sampling Grid

Female grizzly bear density surface models were applied using the most supported baseline detection model (Table 6 with full listing in Appendix 4). A model with year-specific densities (Model 23) was less supported than a constant model (Model 22). However, a model with period (Model 21: 2013-2014 vs. 2019-2020) showed slightly higher support than the constant model. Of the landcover models, a model with deciduous (decid), shrub, and herbaceous (herb) (Model 15) was most supported. Models that had mortality terms (Models 16-18) had less support than the landcover alone model. Various road impact models were considered including straight additive models (Models 3, 7, 9 and 11), implying that density was different near the road pre- and post-road and interaction models with period (Models 8, 10 and 12) suggesting a change in density occurred with the road. In addition, models with road effects only occurring post-road (Model 14) or pre-road (Model 19) were evaluated. Of models considered, a straight additive spline model was most supported (Model 1), suggesting variation in density as a function of distance to road that did not change pre- and post-road. A model with yearly mortality had marginal support (Model 2). None of the interaction models with period showed support suggesting no significant change in female density pre- and post-road.

Table 26. Female spatially explicit density surface modeling model selection results. A base model (g_0 (bk), sigma (.)) was used for all analyses except when noted. An exponential relationship between covariates and density was assumed except where noted. The base model (with no density covariates) is shaded in grey. Sample size adjusted AIC_c, the difference in AIC_c between the most supported model for each model (ΔAIC_c), AIC_c weight (w_i), number of model parameters (K) and log-likelihood (LL) are given. A full list of landcover and mortality models considered is given in Appendix 4.

No	Landcover	Road/Temporal	Mortality	AIC_c	ΔAIC_c	w_i	K	LL
1	decid + shrub + herb	spline(df=3)		2,471.3	0.00	0.36	9	-1,226.2
2	decid + shrub + herb	spline(df=3)	MortsYr	2,473.1	1.73	0.15	10	-1,225.9
3	decid + shrub + herb	Period+spline(df=3)		2,473.5	2.20	0.12	10	-1,226.1
4	decid + shrub + herb	ZOIHR		2,474.0	2.62	0.10	8	-1,228.6
5	decid + shrub + herb	ZOIsig		2,475.1	3.80	0.05	8	-1,229.2
6	decid + shrub + herb	StrataHR		2,475.2	3.87	0.05	8	-1,229.2
7	decid + shrub + herb	spline(df=3)+Period	MortsYr	2,475.3	3.98	0.05	11	-1,225.9
8	decid + shrub + herb	Period*ZOIHR		2,476.1	4.78	0.03	9	-1,228.5
9	decid + shrub + herb	Period+ZOIHR		2,476.1	4.80	0.03	9	-1,228.6
10	decid + shrub + herb	Period*ZOIsig		2,477.3	5.97	0.02	9	-1,229.1
11	decid + shrub + herb	Period+ZOIsig		2,477.3	5.97	0.02	9	-1,229.1
12	decid + shrub + herb	Period*spline(df=3)		2,479.2	7.90	0.01	13	-1,225.6
13	decid + shrub + herb	Period*Strata		2,481.8	10.45	0.00	11	-1,229.1
14	decid + shrub + herb	spline(Post-road,df=3)		2,485.5	14.19	0.00	9	-1,233.3
15	decid + shrub + herb			2,485.9	14.53	0.00	7	-1,235.6
16	decid + shrub + herb		MortsYr	2,487.4	16.10	0.00	8	-1,235.3
17	decid + shrub + herb		Morts10	2,487.7	16.41	0.00	8	-1,235.5
18	decid + shrub + herb		Morts3yr	2,487.8	16.48	0.00	8	-1,235.5
19	decid + shrub + herb	spline(Pre-road,df=3)		2,487.2	15.90	0.00	9	-1,234.1
20	decid + shrub + herb	Period		2,488.0	16.67	0.00	8	-1,235.6
21	Period			2,585.4	114.03	0.00	5	-1,287.5
22	constant			2,587.4	116.03	0.00	6	-1,287.4
23	year			2,589.2	117.82	0.00	7	-1,287.3

Plots of landcover covariates suggest a negative relationship of density with shrub, herbaceous and deciduous landcover. Of covariates considered, deciduous was the strongest predictor of density (Figure 8).

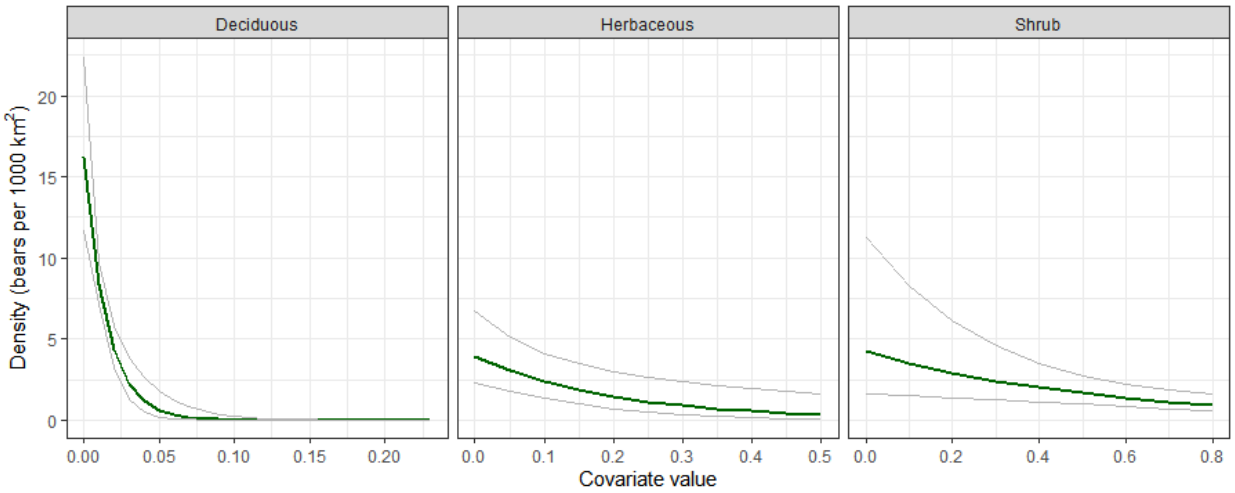

Figure 32. Predicted change in density as a function of landcover covariates for female grizzly bear.

A plot of predicted density on the DNA grid indicates higher densities for the northwestern part of the sampling grid with intermittent areas of higher density in the central area of the grid (Figure 9). The landcover alone model predicts slightly lower densities near the road and in the southeastern portion of the study area. The effect of the spline road term is not large with a slight reduction of densities in the proximity of the road. However, this effect occurred prior to and after the road suggesting pre-existing lower densities in this area.

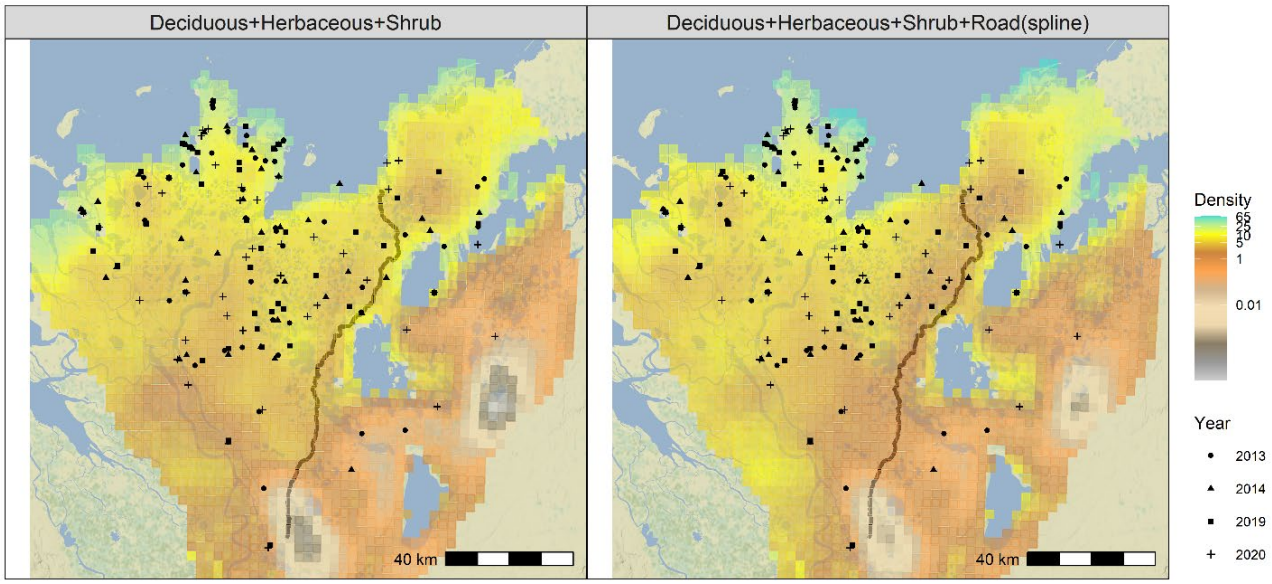

Figure 33. Predicted female grizzly bear density from the most supported density surface models. Also shown are estimated home range centers for each year in the analysis.

Male SECR Analysis

Base SECR Analysis

Models that considered year-specific, session-specific, and behavioural response to sites were considered in the male SECR analysis (Table 7). As with females, a model with site-

specific behavioural response to detection at home range center with a constant σ value was most supported.

Table 27. Male spatially explicit model selection with models indicated by assumptions made about density, detection at home range center (g_0) and scale of movement (σ). Model notation includes: b = change in detection if the bear was detected previously (in any session), B = change in behaviour of bear in previous session to detection. bk = where bears are more or less likely to visit a site after it has been previously visited, constant = single value for parameter. Sample size adjusted AIC_c, the difference in AIC_c from the most supported model (ΔAIC_c), AIC_c weight (w_i), number of model parameters (K) and log-likelihood are given.

No	Density	Detection (g_0)	Scale (σ)	AIC_c	ΔAIC_c	w_i	K	LL
1	constant	bk	constant	1,648.27	0.00	0.87	4	-819.9
2	year	bk	year	1,649.62	1.35	0.06	7	-817.2
3	constant	bk	year	1,653.80	5.53	0.05	7	-819.3
4	constant	bk*year	constant	1,656.63	8.35	0.03	10	-817.2
5	constant	bk+year	year	1,659.96	11.68	0	10	-818.8
6	constant	B	constant	1,697.17	48.90	0	4	-844.4
7	constant	B+year	constant	1,702.49	54.21	0	7	-843.7
8	year	B+year	constant	1,703.73	55.46	0	10	-840.7
9	constant	constant	constant	1,703.00	54.73	0	3	-848.4
10	year	b	constant	1,705.64	57.37	0	7	-845.2
11	year	b	constant	1,705.72	57.45	0	7	-845.3
12	year	year	constant	1,708.21	59.94	0	9	-844.2
13	constant	year	constant	1,708.18	59.91	0	6	-847.7
14	year	constant	year	1,709.52	61.25	0	9	-844.8
15	constant	constant	year	1,709.14	60.87	0	6	-848.1
16	year	b+year	constant	1,710.60	62.33	0	10	-844.1
25	constant	b+year	constant	1,710.28	62.01	0	7	-847.6

A plot of detection rates revealed a similar pattern as females with site-detection rates increasing after initial use of a site (Figure 10). Estimates of g_0 were 0.05 and 0.27 at initial and subsequent detection with the spatial scale parameter (σ) of 11,157.7 meters defining the scale of movement.

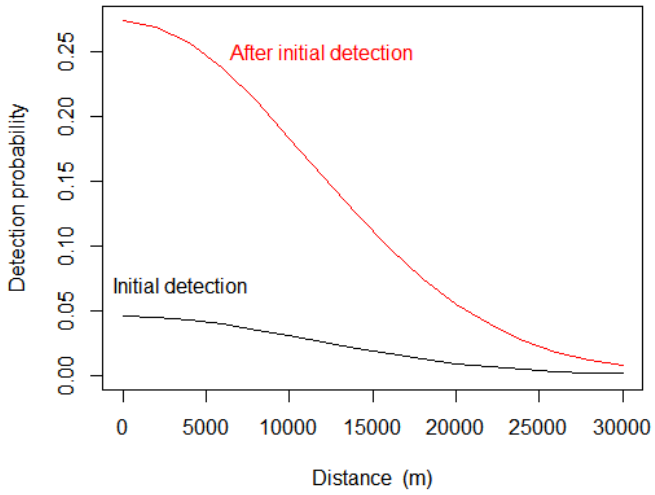

Figure 34. The effect of initial detection on g_0 from model 1 (Table 7).

Estimated home range center displays higher numbers of bears in the northwest of the study area, however, the distribution seemed to even out in 2019-2020 with more bears in the southern portion of the study area (Figure 11).

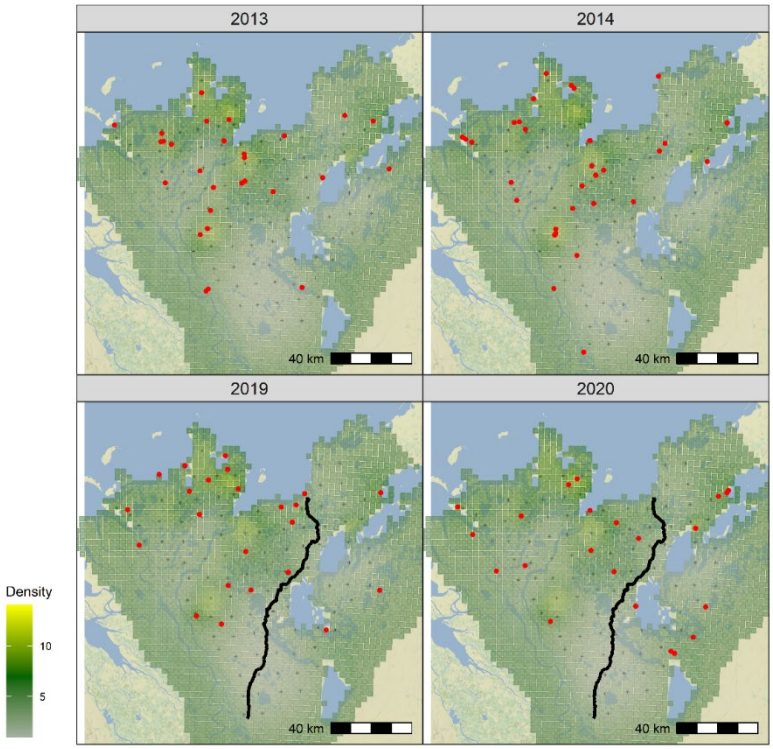

Figure 35. Estimated home range centers and areas of male bears from the most supported baseline SECR model. Relative density based on home range centers is also depicted.

Variation in Density on Sampling Grid

Initially, temporal variation was tested in the data set with a model that had density varying with period (Table 8, Model 27), showing higher support than year-specific densities (Model 29). Of the landcover models, a model with deciduous landcover was most supported (Model

18). Various temporal and road-response models were considered with a model that had interaction of ZOI (at the home range scale) and period being most supported (Model 1). The interaction term was weak as indicated by close support of an additive model (Model 2). A model with a ZOIHR for just the pre-road period showed some support (Model 3) with minimal support for strata-based road effect models (Model 22) or spline-based road models (Models 7, 9 and 10). Mortality covariates (based on cumulative mortality in the previous three years) in addition to road effects (Model 4) had partial support, however, mortality + landcover model had minimal support (Models 20, 21 and 26).

Table 28. Male spatially explicit density surface modeling model selection results. A base model (g_0 (B), sigma (.)) was used for all analyses except when noted. The base model (with no density covariates) is shaded in grey. Sample size adjusted AIC_c, the difference in AIC_c between the most supported model for each model (ΔAIC_c), AIC_c weight (w_i), number of model parameters (K) and log-likelihood (LL) are given. A full list of landcover models considered is given in Appendix 4.

No	Landcover	Road	Mortality	AICc	ΔAIC_c	w_i	K	LL
1	decid	ZOIHR*period		1,609.37	0.00	0.18	7	-797.1
2	decid	ZOIHR+period		1,609.86	0.48	0.14	7	-797.4
3	decid	ZOIHR (pre-road)		1,610.13	0.75	0.12	6	-798.6
4	decid	ZOIHR*period	Morts3yr	1,610.82	1.45	0.09	8	-796.7
5	decid	ZOIHR*period	Morts10yr	1,610.97	1.60	0.08	8	-796.7
6	decid	ZOIHR*period	MortsYr	1,611.09	1.71	0.08	8	-796.8
7	decid	spline(Road,df=4)		1,611.46	2.09	0.06	8	-797.0
8	decid	ZOIHR		1,612.59	3.22	0.04	6	-799.9
9	decid	spline(Road,df=4)		1,612.79	3.41	0.03	8	-797.7
10	decid	spline(Road,df=4)*Period		1,613.01	3.63	0.03	11	-794.1
11	decid	Period		1,613.04	3.66	0.03	6	-800.1
12	decid	spline(Roadpre.df=4)		1,613.43	4.06	0.02	8	-798.0
13	decid	ZOIHR*year		1,614.07	4.70	0.02	9	-797.1
14	decid	ZOI (post-road)		1,614.35	4.98	0.01	6	-800.8
15	decid	spline(Road,df=3)*Period		1,614.80	5.42	0.01	9	-797.5
16	decid	ZOIsig		1,615.25	5.88	0.01	7	-800.1
17	decid	spline(Road,df=3)		1,615.81	6.44	0.01	7	-800.3
18	decid			1,616.13	6.76	0.01	5	-802.8
20	decid		Morts3yr	1,617.37	7.99	0.00	6	-802.3
21	decid		MortsYr	1,617.38	8.01	0.00	6	-802.3
22	decid	StrataHR*Period		1,617.51	8.13	0.00	9	-798.8
23	decid	Year		1,617.58	8.21	0.00	8	-800.0
24	decid	ZOIsig*Period		1,617.93	8.55	0.00	7	-801.4
25	decid		Morts0yr	1,617.97	8.60	0.00	6	-802.6
26	decid	Spline(Roadpost)		1,617.99	8.61	0.00	8	-800.3
27		Period		1,645.13	28.47	0	5	-817.3
28	constant			1,648.27	38.90	0.00	4	-819.9
29		Year		1,649.62	40.25	0.00	7	-817.2

Plots of male density versus deciduous habitat revealed a similar relationship with females with declining density as deciduous cover increased (Figure 12).

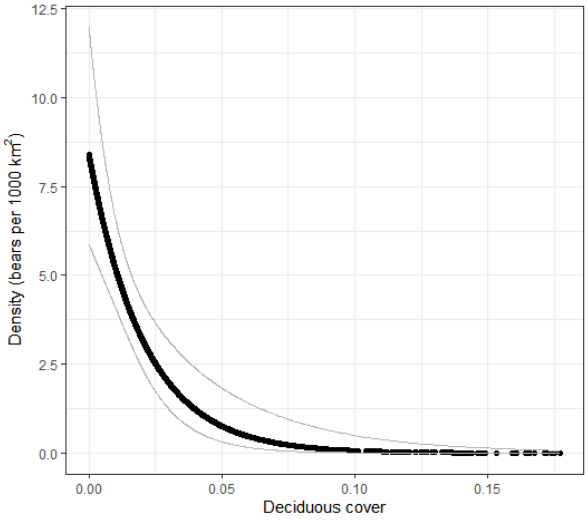

Figure 36. Predicted density of male grizzly bears as a function of deciduous habitat from Model 1 and deciduous and wet herbaceous habitat (Model 2, Table 8). Density is expressed in bears per 1,000 km^2.

A plot of the ZOI pre- and post-road density from the ZOIHR model (Figure 13) suggests a larger gradient in density as a function of distance from road for 2013-2014, however, this effect could be partially due to the higher densities at that time which is suggested by support of an additive model (Model 2). As discussed later, these results suggest a pre-existing density gradient relative to the road with minimal suggestion of increased road effects or potentially a mixed road effect (attraction to the road offsetting increased mortality pressure).

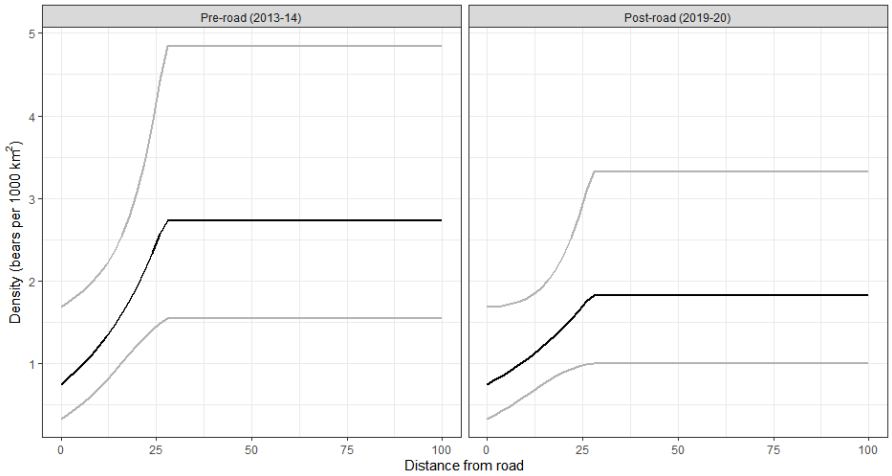

Figure 37. Predicted density of grizzly bears as a function of period and distance from road. The ZOI was based on estimated home-range radius from σ values estimated by SECR analysis. Deciduous landcover was set at mean values (0.035) for mask points that fell within the home-range based ZOI.

Predictions from the deciduous habitat model (Model 1) were plotted and compared with SECR estimated home range center locations from each year sampled (Figure 14). As with females, higher densities were predicted in the northern part of the grid which also corresponded in general to the home range centers (Figure 11). Hot spot areas indicated in Figure 14 had moderate densities predicted but not higher densities suggesting that, as with females, these areas may correspond to ephemeral food resources not well described by landcover.

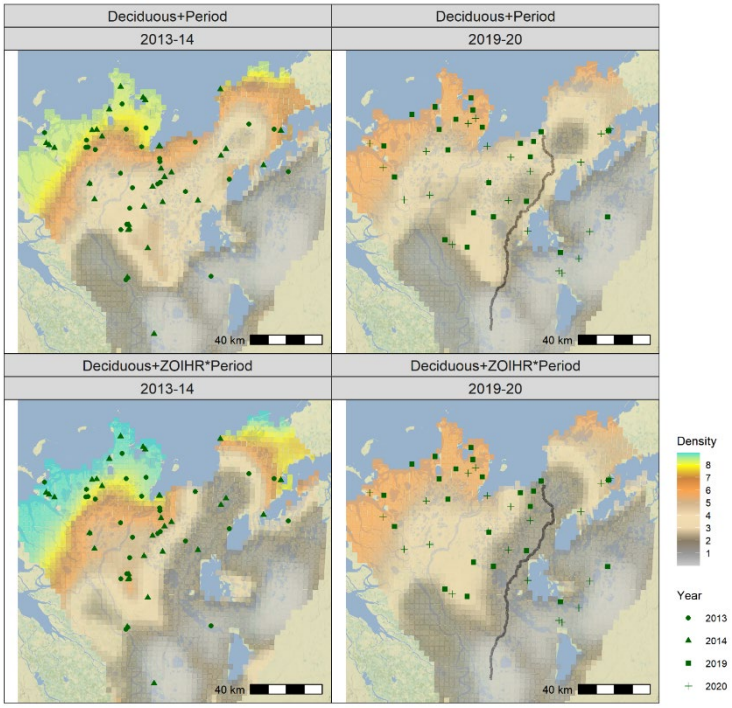

Figure 38. Predicted densities for the most supported landcover model (deciduous) and most supported landcover + road (deciduous ZOIHR*period) models.

The effect of mortalities was explored by plotting estimates from Model 4 where densities were affected by mortalities that occurred in the past three years (Figure 15). When compared with Figure 14 (the same model without the morality term) a slight reduction of density can be seen where mortalities occurred (red stars in Figure 14) over the past three years, especially in 2019-2020 (which had higher mortalities).

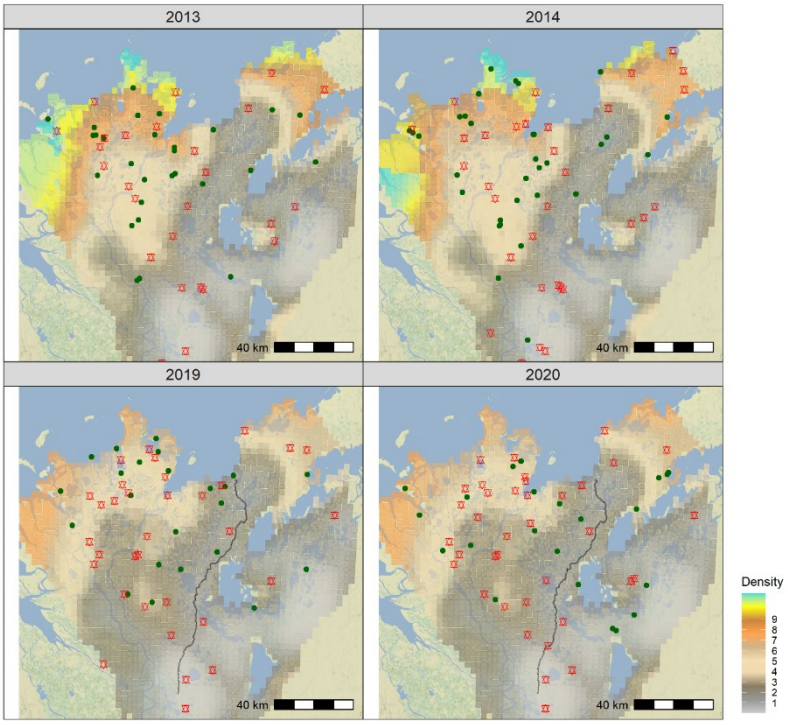

Figure 39. Predictions of most supported landcover + road + mortality model (Model 3: deciduous + ZOIHR*period + morts3yr). Also shown are estimated home range centers (green dots) and mortality locations for the preceding three years before the study (red stars).

Estimates of Abundance and Density

The DNA Grid Area

An initial estimate of bears on the DNA grid area (Figure 1) was derived by models that allowed yearly density estimates for male and female bears. In both analyses, these models were less supported than a constant density model, however, for males, a period model was supported, suggesting a change in density based upon pre- and post-road grouped years (2013-2014 vs. 2019-2020). More precisely, mean male density for pre-road (2013-2014) and post-road (2019-2020) periods was 3.86 (CI=3.03-4.92) and 2.73 (CI=2.09-3.57) bears per 1,000 km^2. For females, mean density was 5.73 (CI=4.76-6.90) and 5.82 (CI=4.86-6.96) for pre- and post-road periods. The combined male and female density estimate for pre- and post-road periods was 9.6 (CI=8.94-10.28) and 8.55 (CI=7.69-9.17) bears per 1,000 km^2.

Regardless, these estimates provide a non-constrained estimate of yearly density and abundance on the sampling grids (Table 9, Figure 16). Estimates of density and abundance suggest female populations were relatively stable, whereas males had a moderate declining trend of approximately 5% per year. The overall abundance trend was decreasing at a rate of approximately 2% per year due to the influence of males. The topic of trend was looked at in more detail in the open model analysis.

Table 29. Estimates of average number of bears on the sampling grid (N) and density (D: bears per 1,000 km^2) for females, males, and females + males as a function of the year of study and underlying density model. A model with yearly estimates of density was used with the most supported detection model for both sexes. The mask areas for the DNA grid perimeter were used for density estimates.

Year	n	N	SE	95% Conf. Limit		CV	D	SE	Conf. Limit	
Females										
2013	46	57.9	7.2	45.4	73.9	12.5%	6.05	0.76	4.74	7.72
2014	45	52.1	6.4	41.0	66.3	12.3%	5.44	0.67	4.28	6.92
2019	49	56.8	6.7	45.0	71.6	11.9%	5.93	0.70	4.71	7.48
2020	47	54.5	6.6	43.1	69.0	12.1%	5.69	0.69	4.50	7.21
Males										
2013	29	36.6	6.0	26.6	50.3	16.3%	3.82	0.62	2.78	5.25
2014	32	37.3	5.7	27.6	50.3	15.4%	3.89	0.60	2.89	5.25
2019	23	26.7	4.7	19.0	37.6	17.5%	2.79	0.49	1.98	3.93
2020	22	25.6	4.6	18.1	36.2	17.9%	2.67	0.48	1.89	3.78
Females + Males										
2013	75	94.5	9.4	77.8	114.7	9.9%	9.87	0.98	8.13	11.99
2014	77	89.4	8.6	74.1	107.9	9.6%	9.34	0.90	7.74	11.27
2019	72	83.5	8.2	68.9	101.2	9.8%	8.73	0.86	7.20	10.57
2020	69	80.1	8.0	65.8	97.4	10.0%	8.37	0.84	6.88	10.17

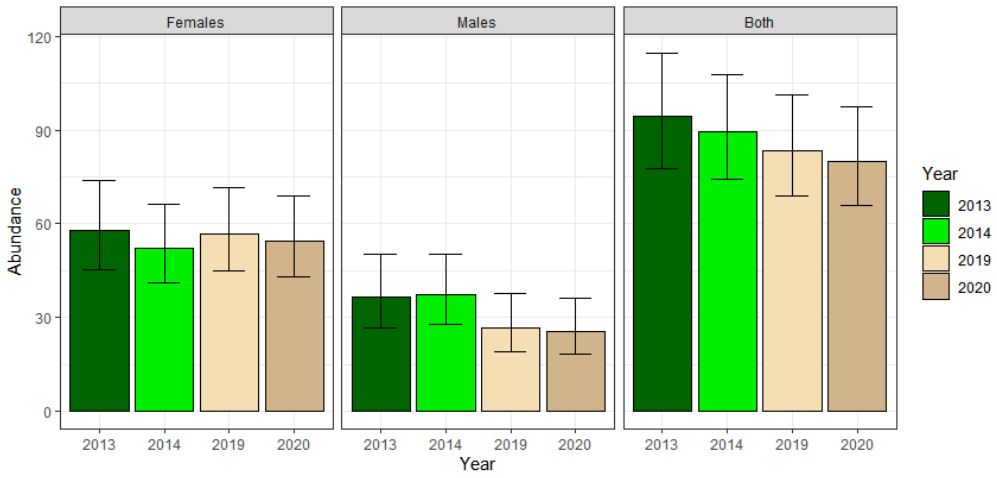

Figure 40. Year-specific abundance estimates for grid area.

Regional Estimates of Population Size for Road and Control Strata

Regional population size estimates were generated for areas within 19.9 and 27 km of the proposed road which was the buffer distance estimated for females and males respectively. These estimates correspond to the average number of bears that would be within 19.9-27 km of the road at any one time (Table 10, Figure 17). Regional estimates were also generated for areas on the DNA grid outside the road buffers. These could be considered a control area

where bear density would be less likely to be influenced by the road. We note that average population size and density was estimated only for areas within the 2014 DNA grid (Figure 1) and not areas beyond the grid boundary such as areas south of Inuvik. This is a conservative approach that ensures that areas where bears are estimated are in the vicinity of tripod sampling sites. Precision of estimates as indexed by coefficient of variation suggested reasonable precision (CVs less than 20%) for all estimates.

Table 30. Estimate of abundance (N) and density (D) for road and control zones for males and females in pre- and post-road periods. The most supported landcover/road models were used for estimates.

Period	Region	N	SE	Conf limit		CV	D	SE	Conf limit	
Females (LC+Period+spline road)										
Pre-road	Road zone	16.1	2.5	11.8	21.9	15.8%	2.04	0.32	1.50	2.78
Post-road	Road zone	16.5	2.6	12.2	22.3	15.5%	2.09	0.32	1.54	2.83
Pre-road	Control	35.9	4.0	29.0	44.6	11.0%	10.04	1.11	8.09	12.45
Post-road	Control	36.7	4.0	29.7	45.4	10.8%	10.26	1.11	8.30	12.67
Males										
Pre-road	Road zone	17.2	2.7	12.6	23.4	15.9%	2.18	0.35	1.60	2.97
Post-road	Road zone	13.4	2.2	9.7	18.6	16.7%	1.70	0.28	1.23	2.35
Pre-road	Control	22.2	3.2	16.8	29.3	14.3%	6.19	0.88	4.68	8.18
Post-road	Control	14.8	2.4	10.8	20.3	16.3%	4.13	0.68	3.01	5.68
Both										
Pre-road	Control	58.1	5.1	49.0	68.9	8.7%	16.23	1.42	13.68	19.25
Post-road	Control	51.5	4.7	43.2	61.5	9.0%	14.39	1.30	12.06	17.17
Pre-road	Road zone	33.3	3.7	26.8	41.5	11.2%	4.23	0.47	3.39	5.26
Post-road	Road zone	29.9	3.4	23.9	37.3	11.4%	3.79	0.43	3.03	4.73

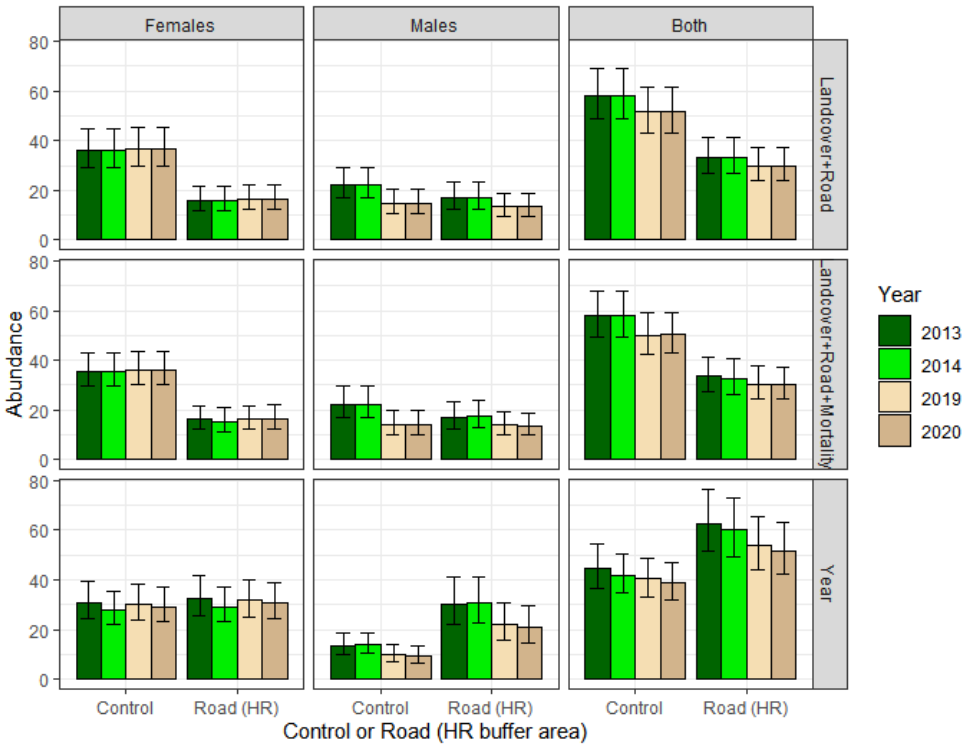

Figure 41. Estimates of average number of bears within control and road zones for SECR models. The Year model assumes constant spatial density and is presented for comparison with the landcover models.

The average number of bears will be affected by differing areas of the road buffer and control areas and therefore a more direct comparison can be gained by comparison of density of bears in each area (Figure 18).

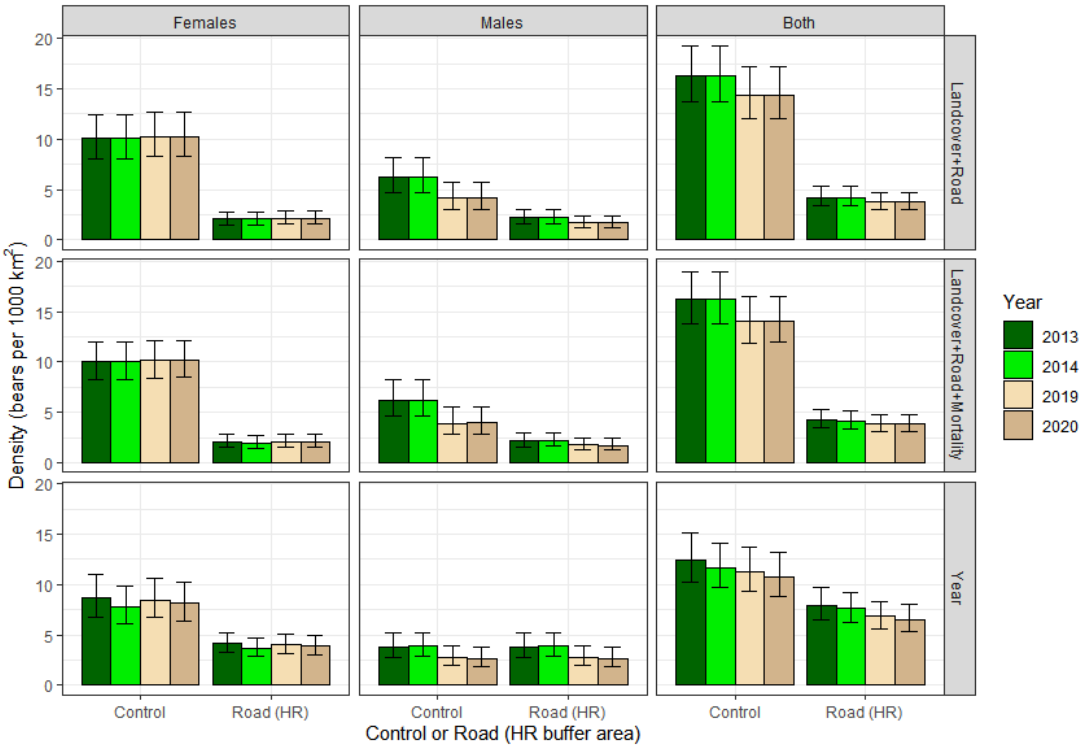

Figure 42. Estimates of density (bears per 1,000 km^2) for road and control area for various supported SECR models. The Year model assumes constant spatial density and is presented for comparison with the landcover models.

Open Model Demographic Analyses

Data Summary

Initial summaries of bears detected each year and redetected in subsequent years reveals that a higher proportion of females were redetected in subsequent years after initial detection when compared to males (Table 11). The question is whether this was due to differences in detection rates, movement off the sampling grid, or survival. The Pradel analysis uses a model-based framework to compare these differences and determine how much they may be attributed to differences in detections compared to demographic differences between years and sexes.

Table 31. Summary of detections, redetections, and new bears for the 2013 and 2014 surveys.

Year	Bears detected	Redetections			Never redetected
		2014	2019	2020	
Females					
2013	46	34	21	14	9
2014	45		21	14	23
2019	49			33	16
2020	47				47
Males					
2013	29	14	2	2	13
2014	32		4	1	27
2019	23			9	14
2020	22				22
Males +Females					
2013	75	48	23	16	22
2014	77		25	15	50
2019	72			42	30
2020	69				69

Movements of Bears between Years of Sampling

Frequencies of yearly detections, which is the number of years that an individual bear was detected were summarized for male and female bears. This summary revealed that 58 of 95 (61%) of females and 28 of 76 (37%) of males were redetected across years (Table 12). The distance moved between estimated home range centers (Figures 7 and 11) for bears detected in more than one year was larger for males than females.

Table 32. Frequencies of yearly detections for male and female bears and mean distances moved between home range centers (for bears detected in more than one year).

Sex	Yearly detections					Distance moved between HR centers				
	1	2	3	4	total	Mean	std	Min	Max	n
Females	37	35	12	11	95	9.7	7.8	0.0	33.2	58
Males	48	26	2	0	76	14.2	12.4	0.0	46.1	28

Plots of movement between home range centers also demonstrate more yearly redetections as well as lower levels of movement between redetections for female bears compared to male bears (Figure 19).

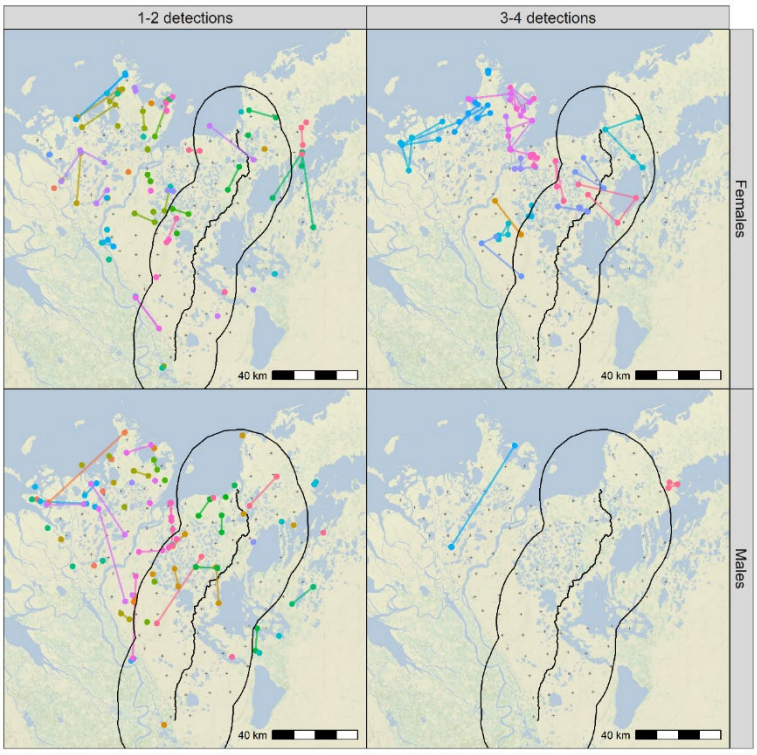

Figure 43. Yearly home range center locations with paths connecting bears that were detected in more than one year. The buffer zone of influence of the road for males and females is shown for reference.

Bear home range centers were classified as being either within or outside buffer areas each year (Table 13), as well as successive movements into and out of buffer areas for bears that were detected in more than one year. In general, the proportion of bear home range centers in the buffer areas remained relatively constant for females but was more variable for males. Bears tended to remain either within or outside the buffer areas, with minimal movement between areas. One issue with this comparison is that the interval between 2014 and 2019 was five years and therefore the 2019 comparison is based on bears detected in 2013 or 2014. Regardless, no large-scale directional trends in movement between control or road area are indicated for either sex.

Table 33. Proportion of bears in road home range buffer areas (females-19.9 km, males-27.3 km) and movements from the previous year into and out of buffer areas (for bears detected in more than one year).

	Home Range Centers in Buffer Areas			Movements from Previous Year			
	control	road	% in road buffer	control-control	control-road	road-control	road-road
Females							
2013	34	12	35%				
2014	34	11	32%	24	3	1	6
2019	37	12	32%	17	1	0	6
2020	36	11	31%	23	2	2	7
Males							
2013	20	9	45%				
2014	19	13	68%	8	1	2	3
2019	14	9	64%	3	0	0	2
2020	16	6	38%	7	0	0	4

Open Model Analysis of Full Study Area

Base detection models were built partially using the results of the SECR analysis that suggested a behavioural response as modeled using a unique recapture term. Models that were considered included: permanent behavioural response (b-once a bear is detected, its detection changes for all remaining sessions), transient behavioural response (B-once a bear is detected, its detection changes for only the next session), and behavioural responses that occurred only within yearly sampling (B_{year}, $b_{session}$) or across all yearly sessions (B and b). For the initial phase of detection model fitting, sex-specific apparent survival and constant additions was assumed. Of models considered, a model with sex-specific transient behavioural response that was constrained to occur withing yearly sessions was most supported (Table 14, Model 2).

Using this base detection model, demographic model with sex- and year-specific estimates of apparent survival and rates of addition were tested. Of models considered, a model with sex-specific apparent survival (ϕ) and rates of addition (f) was most supported (Model 1). In general, there was minimal support for models with year-specific or interactions between year and sex demographic parameters.

Table 34. Pradel model selection results. The parameters of the Pradel model are apparent survival (ϕ), rates of addition (f), detection probability (p). Covariate behaviour terms include: permanent (b-once a bear is detected its detection changes for the remainder of sessions), transient (B-once a bear is detected its detection changes for only the next session). Sample size adjusted AIC_c, the difference in AIC_c between the most supported model for each model (ΔAIC_c), AIC_c weight (w_i), number of model parameters (K) and log-likelihood (LL) are given.

No	Detection (p)	Survival (Φ)	Additions (f)	AIC_c	ΔAIC_c	w_i	K	LL
1	sex*B_{year}	sex	sex	2238.03	0.00	0.39	8	-1110.4
2	sex*B_{year}	sex	constant	2238.09	0.33	0.37	7	-1111.6
3	sex*B_{year}	sex+year	sex	2241.75	3.07	0.06	10	-1110.0
4	sex*B_{year}	sex*year	sex	2241.88	3.19	0.06	10	-1110.0
5	sex*B_{year}	sex	sex+year	2242.38	3.69	0.05	10	-1110.3
6	sex*B_{year}	sex	year	2242.18	3.84	0.04	9	-1111.3
7	sex*B_{year}	sex	sex*year	2245.75	6.25	0.01	12	-1109.6
8	sex*B_{year}	sex*year	year	2245.62	6.55	0.01	11	-1110.7
9	sex*B_{year}	year*sex	constant	2246.08	7.01	0.01	11	-1110.9
10	B_{year}	sex	constant	2246.28	8.95	0.01	5	-1117.9
11	sex*B_{year}	year*sex	year	2249.68	9.72	0.00	13	-1110.3
12	sex*B_{year}	year*sex	year*sex	2254.83	13.21	0.00	16	-1109.0
13	Sex*B	sex	constant	2251.36	13.33	0.00	7	-1118.6
14	sex*b_{year}	sex	constant	2251.60	13.84	0.00	7	-1118.3
15	sex*B_{year}	year	year*sex	2254.42	14.46	0.00	13	-1112.7
16	sex*b	sex	constant	2252.89	15.13	0.00	7	-1119.0
17	sex*b_{year}	sex	constant	2253.51	15.98	0.00	6	-1120.4
18	sex	sex	constant	2254.58	17.25	0.00	5	-1122.0
19	b_{year}	sex	constant	2255.99	18.67	0.00	5	-1122.8
20	sex+year	sex	constant	2261.06	23.03	0.00	8	-1121.9
21	constant	constant	constant	2264.29	27.25	0.00	3	-1129.0
22	sex*t	sex	constant	2267.71	28.65	0.00	11	-1121.7
23	sex*session	sex	constant	2267.71	28.65	0.00	11	-1121.7

A reduced SECR-based Pradel model analysis was applied using the most support closed models (Table 15). The baseline SECR detection model (g_0(sex*bk), σ(sex)) was used to model detection. Various kernel between-year movement models were considered with constant and sex-specific movements. Of models considered, a model with sex-specific between-year movements, and sex-specific apparent survival and rates of additions was most supported; a similar result to the closed model analysis.

Table 35. SECR Pradel model selection. The baseline SECR model (g_0(sex*bk), λ(sex)) model was used for all analyses. Various yearly kernel movement models (Exp=exponential, Norm=Normal, Stationary) were applied. Sample size adjusted AIC_c, the difference in AIC_c between the most supported model for each model (ΔAIC_c), AIC_c weight (w_i), number of model parameters (K) and log-likelihood (LL) are given.

No	Movement	Survival Φ	Additions (f)	AIC_c	ΔAIC_c	w_i	K	LL
1	Exp(sex)	sex	sex	5,969.06	0.00	0.24	12	-2,971.5
2	Exp(.)	sex	sex	5,969.56	0.50	0.19	11	-2,972.9
3	Norm(.)	sex	sex	5,970.00	0.94	0.15	11	-2,973.1
4	Norm(sex)	sex	sex	5,970.61	1.55	0.11	12	-2,972.3
5	Exp(.)	sex	constant	5,970.93	1.87	0.10	10	-2,974.8
6	Norm(.)	sex	constant	5,971.36	2.30	0.08	10	-2,975.0
7	Stationary	sex	sex	5,971.74	2.68	0.06	10	-2,975.2
8	Stationary	sex	constant	5,973.19	4.13	0.03	9	-2,977.0
9	Exp(sex)	sex+year	sex	5,973.45	4.39	0.03	14	-2,971.3
10	Exp(sex)	sex*year	sex	5,978.12	9.06	0.00	16	-2,971.2

Model averaged parameter estimates revealed relatively high apparent survival for females and relatively high rates of addition for males. Addition of apparent survival and rates of addition suggested stable population sizes for females and a declining population of males. However, the level of precision of trend estimates was low and therefore this estimate should be interpreted cautiously with closed models (Table 16). The SECR version produced similar estimates, however, precision of estimates was higher. Both closed and SECR approaches suggest stable female populations with males declining at a rate of 5% per year.

Table 36. Pradel model averaged demographic parameter estimates for the closed and SECR Pradel models in Tables 13 and 14.

Year/sex	Parameter	Closed				SECR			
		Estimate	SE	Conf. Limit		Estimate	SE	Conf. Limit	
Females									
2013-2014	Apparent survival (φ)	0.88	0.04	0.78	0.94	0.89	0.02	0.84	0.93
	Rates of addition (*f*)	0.13	0.09	0.04	0.42	0.12	0.02	0.08	0.18
	Rate of change (λ = φ + *f*)	1.01	0.09	0.82	1.36	1.01	0.03	0.92	1.11
2014-2019	Apparent survival (φ)	0.88	0.02	0.82	0.91	0.89	0.02	0.84	0.93
	Rates of addition (*f*)	0.14	0.03	0.10	0.20	0.12	0.02	0.08	0.18
	Rate of change (λ = φ + *f*)	1.02	0.03	0.92	1.12	1.01	0.03	0.92	1.11
2019-2020	Apparent survival (φ)	0.87	0.04	0.78	0.93	0.89	0.02	0.84	0.93
	Rates of addition (*f*)	0.15	0.04	0.09	0.24	0.12	0.02	0.08	0.18
	Rate of change (λ = φ + *f*)	1.02	0.05	0.87	1.17	1.01	0.03	0.92	1.11
Males									
2013-2014	Apparent survival (φ)	0.79	0.23	0.20	0.98	0.75	0.05	0.65	0.83
	Rates of addition (*f*)	0.18	0.08	0.07	0.43	0.19	0.05	0.12	0.32
	Rate of change (λ = φ + *f*)	0.96	0.24	0.27	1.41	0.95	0.07	0.77	1.15
2014-2019	Apparent survival (φ)	0.77	0.05	0.66	0.84	0.75	0.05	0.65	0.83
	Rates of addition (*f*)	0.19	0.05	0.11	0.30	0.19	0.05	0.12	0.32
	Rate of change (λ = φ + *f*)	0.95	0.07	0.78	1.15	0.95	0.07	0.77	1.15
2019-2020	Apparent survival (φ)	0.76	0.07	0.59	0.87	0.75	0.05	0.65	0.83
	Rates of addition (*f*)	0.19	0.06	0.10	0.35	0.19	0.05	0.12	0.32
	Rate of change (λ = φ + *f*)	0.95	0.09	0.69	1.22	0.95	0.07	0.77	1.15

The estimates from Table 16 can also be viewed graphically which demonstrates that females maintained their population size with higher apparent survival whereas males had lower apparent survival but higher rates of addition (Figure 20). It also illustrates that confidence limits were tighter for the SECR Pradel model.

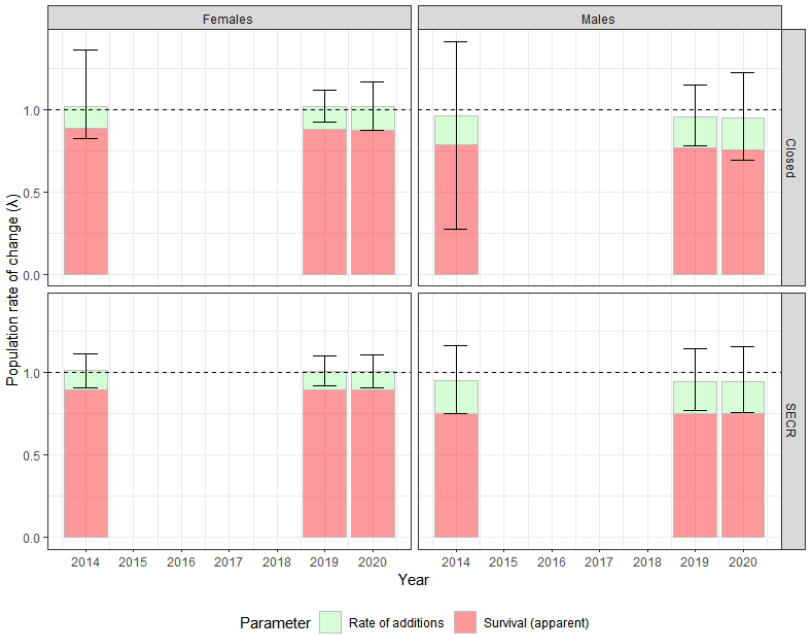

Figure 44. Model averaged estimates of apparent survival (pink), rates of addition (green) and population rate of change (λ) as listed in Table 16. Each year refers to the interval preceding the year (i.e., 2014 indicates the interval from 2013-2014).

Estimation of Demographic Differences between Road and Control Buffer Areas

To test for road and control buffer effects, the estimated home range centers (Figure 19, Table 13) were used to assign strata to individual bears each year as well as estimate distance from the road for each year. These were then used as individual covariates for ϕ and f. The most supported full study area model (ϕ(sex), f(sex), p($B_{session}$*sex)) was used as a baseline for the analysis. Road effect terms (strata and distance from road) were entered as additive and interaction terms in a similar way as the density surface model analysis. A period term that compared demographic estimates between the 2013-2014, 2014-2019 and the 2019-2020 interval was used to assess if demographic rates changed when the road was open. We note that the road opened to traffic in November of 2017, and therefore the majority (three years) of the 2014-2019 interval was with the road closed. The SECR-based open model does not allow individual covariate terms and therefore the closed Pradel model was used for this analysis.

Model selection results suggested minimal impacts of the road (as defined by HR-based strata and distance from road) on apparent survival and rates of addition (Table 17) with no road-effect model showing higher support than the baseline demographic model. Some models that estimated strata-specific effects showed some support (as indicated by ΔAIC_c terms of <2), however only one of the strata*Period models was supported: Model 4, which suggested a slight effect of the road on rates of addition, suggesting these effects were not necessarily due to implementation of the road. Models with year-specific interactions between demographic parameters and the road/control area did not converge which was likely due to parameter identifiability and sparse sample sizes of bears detected in the road area alone (Table 13).

Table 37. Model selection for Pradel analysis of road effects. Closed SECR models were used with base detection model (p(sex*$B_{session}$)). The most supported model for the study area (ϕ(sex), f(sex)) was used as a baseline model for the analysis.

No	Apparent Survival (φ)	Rates of Addition (*f*)	AIC_c	ΔAIC_c	w_i	K	LL
1	sex	sex	2,270.17	0.00	0.26	8	-1,126.63
2	sex+Strata	sex	2,271.70	1.53	0.12	9	-1,126.27
3	sex	sex+Strata	2,272.03	1.86	0.10	9	-1,126.44
4	sex+Strata	sex+Strata:Period	2,272.13	1.96	0.10	11	-1,124.21
5	sex	sex*Strata	2,272.20	2.03	0.10	11	-1,124.24
6	sex+log(distroad)	sex	2,272.26	2.09	0.09	9	-1,126.55
7	sex+Strata:Period	sex+Strata:Period	2,273.50	3.33	0.05	12	-1,123.73
8	sex+Strata:Period	sex	2,273.66	3.49	0.05	10	-1,126.12
9	sex+Strata	sex+Strata	2,273.85	3.69	0.04	10	-1,126.22
10	sex+Strata	sex+strata*Period	2,274.18	4.01	0.04	12	-1,124.07
11	sex+Strata:Period	sex	2,274.91	4.74	0.02	11	-1,125.60
12	sex+Strata		2,275.60	5.43	0.02	11	-1,126.27
13	sex*Strata	sex	2,276.26	6.09	0.01	10	-1,126.27
14	sex*Period*log(distroad)	sex	2,276.56	6.39	0.01	9	-1,128.70
15	sex*Period*strata	sex	2,280.51	10.34	0.00	11	-1,128.40

Inspection of model averaged estimates reveals similar trends for road and control strata with a decline in males suggested (λ<1) and stable populations of females in both road and control strata (Figure 21). A slight decrease in rates of additions is suggested for the 2019-2020 interval, however, the precision of estimates is low, limiting the ability to interpret this trend.

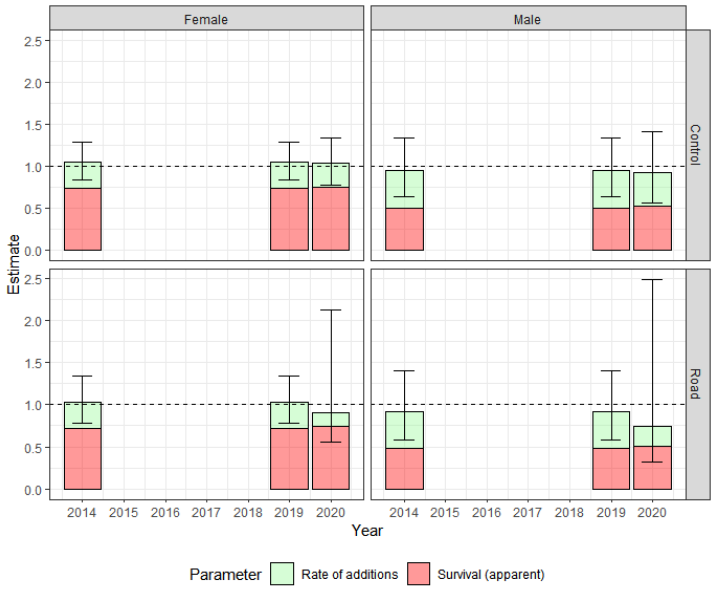

Figure 45. Model averaged estimates of demographic parameters by HR road buffer strata based on models in Table 18.

DISCUSSION

The main objectives of this study were to assess if grizzly bear density and distribution were potentially influenced by the ITH. Field sampling detected a sufficiently large population of bears to allow precise estimates of density and abundance with coefficients of variation less than 20% for treatment and control areas.

We used a variety of SECR-based density surface model analyses to estimate potential changes in density in male and female bears relative to the road. No change in density following the implementation of the road could be detected, however, pre-existing density gradients relative to the road were evident. A similar trend appeared in the open model analysis of road and control strata.

The combined male and female density estimates for the pre- and post-road periods were 9.6 (CI=8.94-10.28) and 8.55 (CI=7.69-9.17) bears per 1,000 km^2. Grizzly bear densities above the tree line are generally between 4-10 bears/1,000 km^2 (e.g. Poole and Setterington 2012, Dumond et al. 2015, Jessen 2017, Species at Risk Committee 2017). Grizzly bear density near the highway was 4.2 (CI=3.4-5.3) and 3.8 (CI=3.0-4.7) bears/1,000 km^2 (before and after road opening), which is comparable to these other studies. Notably, the control area had a bear density of 16.2 (CI=13.7-19.3) and 14.4 (CI=12.1-17.2) bears/1,000 km^2 (before and after road opening), which is high for barren ground grizzly bears (the next highest being 10.5-12 bears/1,000 km^2 for the coastal region of the Yukon North Slope, which is within 200 km of our study area).

The use of density as a response variable to development is potentially compromised by likely mechanisms that might change density relative to the road. Namely, roads might potentially attract bears if roadkill or other attractants are produced by the road. Some studies have also suggested that males might avoid roads due to mortality pressure which may make females with cubs more likely to use road areas (Graham et al. 2010, Boulanger and Stenhouse 2014). Also, potential reductions in density due to increased mortality relative to the road occur at a longer time scale than the present study that was conducted two to three years after the road was implemented. As of 2021, there have been no reported traffic-related mortalities of grizzly bears along the highway, and spatial patterns of grizzly bear harvest do not appear to be affected by the highway (d'Eon-Eggertson 2023).

One of the most direct impacts to density and variation in density in the study area is direct mortality and therefore we considered mortality locations as part of the density surface analysis. We found only weak correspondence of changes in density with mortality pressure suggesting that the spatial dynamics of bears in the study area is dynamic and the level of mortality is low enough that an actual shift in density was not detectable due to mortality risk.

We detected a 5% yearly decline in the male segment of the population, in contrast with a relatively stable overall bear population. Using estimates of abundance for the sampling grid (Table 9), we estimated the proportion of males that were known mortalities each year, which varied from 5.5% (2 mortalities/36.6 bears) in 2013 to 39.1% (10 mortalities/25.6 bears) in 2020. These levels of mortality may be contributing to a reduced survival rate (apparent survival 0.76-0.79) which is not being fully offset by additions (0.18-0.19 per year), leading to an overall decline in male bear abundance. In contrast, female mortalities

were lower ranging from 5.2% (3 mortalities/57.9 bears) in 2013 to 1.85% (1 mortality/54.5 bears) in 2020. Apparent survival was higher (0.88) and therefore the population was stable given a rate of addition of 0.13-0.14 per year. A challenge with estimating the proportion of harvest is defining the "vulnerable population" given that it is likely there is movement of bears from other areas each year which can offset mortalities.

The main limitation of this study is the relatively short time interval between the opening of the road (at the end of 2017) and sampling in 2019 and 2020. For the open model analysis, this meant that there was only one survey interval (2019-2020) to assess survival when the road was fully open, given that the road was only open for a portion of the previous 2014-2019 interval. This relatively short period means that the ability to detect a likely change in density will be limited by sample sizes, given that usual demographic responses of bears to development involve smaller scale incremental changes in survival as well as changes in distribution (Proctor et al. 2002, Proctor et al. 2005, Boulanger et al. 2018).

Density Surface Models

The density surface models in this analysis are reasonably simplistic in that only one or two habitat features are associated with density. This is presumably due to sample size limitations as well as the relatively large scale of habitat selection of grizzly bears detected by DNA sampling. One important point to note is that associations with habitat variables such as deciduous (closed birch) habitat most likely represent gradients of habitat selection rather than selection for the single factor. For example, principal component analysis results suggests that deciduous (closed birch) habitat is negatively related with sparse vegetation and non-vegetated areas, so negative association with this habitat type also could infer positive selection for the sparse/non-vegetated habitat types (Appendix 2). It is also possible that ephemeral food sources not indicated by habitat covariates such as caribou, Arctic char, whitefish or marine resources may influence grizzly bear distribution as suggested by previous studies (Edwards et al. 2010). Stable isotope analysis of hair samples might provide a way to assess if bears are relying more on marine resources as was done in Edwards et al. 2010. Current caribou locations suggest few caribou are on the sampling grid during the time of the survey. There is however a privately-owned reindeer herd that spends the summer on Richards Island (the portion of the study area with the highest bear densities), and reindeer were often seen there during the survey. Finally, current distribution could also be influenced by historic mortality events as well as the location of cabins in the survey area.

The presence of a site-specific behavioural response with detection rates increasing after subsequent capture has been detected in numerous northern grizzly bear populations using posts (Government of Nunavut unpublished data). This model makes intuitive sense biologically. Once a site has been "discovered" it is likely it will be revisited.

It is possible that the spatial scale of movements of bears might change in response to the road, or that the road may not actually influence densities of bears in the entire 19.9-27.3 km strata buffer zone (Table 11). Results from the male analysis suggest a graduated change in density with distance from road, however, this effect was present for both pre- and post-road survey years, suggesting that either the path of the road had previous impacts on male bear density or that there were other features that influenced density which were not included in the density surface model.

We also note that mortality of bears could actually increase beyond the HR buffer zones if the road provides enhanced access for hunters to travel beyond the immediate area of the road. In this case, the "ZOI" of the road may not simply be defined as HR zone. For this reason, we also considered spline models that did not constrain the effect of the road to be within a single home range radius. This model was supported with females, however, there again was no suggested impact of the road which would be suggested by a significant interaction term of period and distance from road.

Future Research

One limitation to the current open model analysis is that there was only one interval (2019-2020) where the road was fully open which compromised the ability to detect changes in demographic parameters. More sessions of sampling would help offset this issue. Power analyses could be conducted to assess optimal sampling intervals for future surveys. One simple approach is determination of power to assess a given level of change in two density estimates which can be solved using closed-form equations (Efford and Boulanger 2019).

Open mark-recapture models that allow incorporation of known mortalities could be applied to the data set (Barker and White 2001). This would add sessions for 2015, 2016, 2017, and 2018 in addition to the existing DNA-based sessions. The model would be constrained to allow harvest data for each of the years of the analysis. This would potentially provide enhanced estimates of survival.

Density surface models were unable to fully explain the clustering of bears in the northwestern section of the sampling grid. One potential explanation is the attraction of marine resources in this area (Edwards 2009, Edwards et al. 2009, Edwards et al. 2010). Stable isotope analysis of hairs provides one potential method to further assess if bears in this area are utilizing marine or other resources unique to this part of the Mackenzie River Delta.

LITERATURE CITED

Barker, R.J. and G.C. White. 2001. Joint analysis of live and dead encounter of marked animals. Pages 361-366 *in* R. Fields, R.J. Warren, H. Okarma and P.R. Seivert, editors. Intergrating People and Wildlife for a Sustainable Future: Proceedings of the Second International Wildlife Management Congress. The Wildlife Society, Bethesda Md., Gödölló, Hungary.

Boulanger, J. 2013. An analysis of the 2012 Izok grizzly bear DNA mark-recapture data set, Unpublished Report for MMG Resources.

Boulanger, J., R. Baron and H. Sawada. 2014. Inuvik-Tuktoyaktuk highway 2013 grizzly bear DNA inventory: Estimates and density surface modelling. Environment and Natural Resources, Government of the Northwest Territories.

Boulanger, J. and M. Branigan. 2020. Inuvik-Tuktoyaktuk highway 2013 and 2014 grizzly bear DNA inventory: Estimates and density surface modeling. Environment and Natural Resources, Government of the Northwest Territories. Manuscript Report No. 288.

Boulanger, J., S.E. Nielsen and G.B. Stenhouse. 2018. Using spatial mark-recapture for conservation monitoring of grizzly bear populations in Alberta Scientific Reports 8:5204, https://rdcu.be/KIfV.

Boulanger, J. and G.B. Stenhouse. 2014. The impact of roads on the demography of grizzly bears in Alberta. PLoS One 9:e115535.

Boulanger, J., G.C. White, B.N. McLellan, J.G. Woods, M.F. Proctor and S. Himmer. 2002. A meta-analysis of grizzly bear DNA mark-recapture projects in British Columbia. Ursus 13:137-152.

Burnham, K.P. and D.R. Anderson. 1998. Model selection and inference: A practical information theoretic approach. Springer, NY.

COSEWIC. 2012. COSEWIC assessment and status report on the Grizzly Bear *Ursus arctos* in Canada. Committee on the Status of Endangered Wildlife in Canada. Ottawa. xiv + 84pp.

d'Eon-Eggertson, F. 2023. Inuvik-Tuktoyaktuk Highway and Harvest. Environment and Natural Resources, Government of the Northwest Territories. Manuscript Report No. 306.

Dumond, M., J. Boulanger and D. Paetkau. 2015. The estimation of grizzly bear density through hair-snagging techniques above the tree line. Wildlife Society Bulletin 39:390-402.

Edwards, M.A., A.E. Derocher, K.A. Hobson, M. Branigan and J. Nagy. 2010. Fast carnivores and slow herbivores: differential foraging strategies among grizzly bears in the Canadian Arctic. Oecologia 165:877-889.

Edwards, M.A.S. 2009. Spatial ecology of grizzly bears (*Ursus arctos*) in the Mackenzie Delta, Northwest Territories, Canada. University of Alberta, Edmonton, AB.

Edwards, M.A.S., J. Nagy and A.E. Derocher. 2009. Low site fidelity and home range drift in a wide-ranging, large Arctic omnivore. Animal Behaviour 77:23-28.

Efford, M. 2004. Density estimation in live-trapping studies. Oikos 106:598-610.

Efford, M. 2019. openCR 1.3 - open population capture–recapture R package.

Efford, M., D.L. Borchers and A.E. Byrom. 2009. Density estimation by spatially explicit capture–recapture: likelihood-based methods. Pages 255-269 *in* D.L. Thompson, E. G. Cooch and M.J. Conroy, editors. Modeling demographic processes in marked populations. Springer, NY.

Efford, M. and J. Boulanger. 2019. Fast evaluation of study designs for spatially explicit capture recapture. Methods in Ecology and Evolution 10:1,529-1,535.

Efford, M., D.K. Dawson and C.S. Robbins. 2004. DENSITY: software for analysing capture-recapture data from passive detector arrays. Animal Biodiversity and Conservation 27:217-228.

Efford, M.G. 2011. Estimation of population density by spatially explicit capture-recapture analysis of data from area searches. Ecology 92:2,202-2,207.

Efford, M.G. 2014a. Bias from heterogeneous usage of space in spatially explicit capture-recapture analyses. Methods in Ecology and Evolution 5:599-602.

Efford, M.G. 2014b. secr spatially explicit capture recapture models. R package version 2.8.1, http://CRAN.R-project.org/package=secr. http://CRAN.R-project.org/package=secr.

Efford, M.G. and D.K. Dawson. 2012. Occupancy in continuous habitat. Esosphere 3:1-14.

Efford, M.G. and R.M. Fewster. 2013. Estimating population size by spatially explicit capture-recapture. Oikos 122:918-928.

Efford, M.G. and M.R. Schofield. 2020. A spatial open-population capture-recapture model. Biometrics:1-11.

Graham, K., J. Boulanger, J. Duval and G. Stenhouse. 2010. Spatial and temporal use of roads by grizzly bears in west-central Alberta. Ursus 21:43-56.

Hastie, T.J. and R.J. Tibshirani. 1990. Generalized additive models. Chapman and Hall, NY.

Huggins, R.M. 1991. Some practical aspects of a conditional likelihood approach to capture experiments. Biometrics 47:725-732.

Jessen, T. 2017. Spatiotemporal factors influencing the distribution and abundance of grizzly bears (*Ursus arctos*) inhabiting the barren-grounds of the central Canadian Arctic. Master's thesis, University of Calgary, Calgary, AB.

Kahle, D. and H. Wickham. 2013. ggmap: Spatial Visualization with ggplot2. The R Journal 5:144-161.

Kendall, K.C., A.C. Macleod, K.L. Boyd, J. Boulanger, J.A. Royle, W.F. Kasworm, D. Paetkau, M.F. Proctor, K. Annis and T.A. Graves. 2015. Density, distribution, and genetic structure of grizzly bears in the cabinet-Yaak ecosystem. The Journal of Wildlife Management 80:314-331.

McGarigal, K., S. Cushman and S. Stafford. 2000. Multivariate statistics for wildlife and ecology research. Springer, NY.

Paetkau, D. 2003. Genetical error in DNA-based inventories: insight from reference data and recent projects. Molecular Ecology 12:1,375-1,387.

Paetkau, D. 2004. The optimal number of markers in genetic capture-mark-recapture studies. Journal of Wildlife Management 68:449-452.

Paetkau, D., R. Slade, M. Burden and A. Estoup. 2004. Genetic assignment methods for the direct, real-time estimation of migration rate: a simulation-based exploration of accuracy and power. Molecular Ecology 13:55-65.

Pebesma, E. 2018. Simple Features for R: Standardized Support for Spatial Vector Data. The R Journal 10:439-446.

Pollock, K.H. and M.H. Otto. 1983. Robust estimation of population size in closed animal populations from capture-recapture experiments. Biometrics 39:1,035-1,049.

Poole, K. and M. Setterington. 2012. Izok Corridor Project: 2012 Wildlife Field Report. Prepared for MMG Resources Inc. by Aurora Wildlife Research (Nelson, BC) and EDI Environmental Dynamics Inc., Whitehorse YT.

Pradel, R. 1996. Utilization of mark-recapture for the study of recruitment and population growth rate. Biometrics 52:703-709.

Proctor, M., B.N. McLellan, J. Boulanger, C.D. Apps, G. Stenhouse, D. Paetkau and G. Mowat. 2010. Ecological investigations of grizzly bears in Canada using DNA from hair: 1995-2005: a review of methods and progress. Ursus 21:169-188.

Proctor, M., B.N. McLellan and C. Strobeck. 2002. Population fragmentation of grizzly bears in Southeastern British Columbia. Ursus 13:153-160.

Proctor, M., B.N. McLellan, C. Strobeck and R. Barclay. 2005. Genetic analysis reveals demographic fragmentation of grizzly bears yielding vulnerably small populations. Proceedings of the Royal Society, London 272:2,409-2,416.

QGIS Foundation. 2020. QGIS Geographic Information System. QGIS Association. www.qgis.org.

R Development Core Team. 2009. R Foundation for Statistical Computing, Vienna, AUT.

Ross, P. I. 2002. Update COSEWIC status report on the grizzly bear *Ursus arctos* in Canada, in COSEWIC assessment and update status report on the Grizzly Bear *Ursus arctos* in Canada. Committee on the Status of Endangered Wildlife in Canada. Ottawa, ON.

Royle, J.A., R.B. Chandler, R. Sollman and B. Gardner. 2014. Spatial capture recapture. Academic Press, Watham, MA.

Royle, J.A., R.B. Chandler, C.C. Sun and A.K. Fuller. 2013. Integrating resource selection information with spatial capture–recapture. Methods in Ecology and Evolution 4:520-530.

Species at Risk Committee. 2017. Species Status Report for Grizzly Bear (*Ursus arctos*) in the Northwest Territories. Species at Risk Committee. Yellowknife, NT.

Species at Risk Public Registry. 2018. Grizzly Bear (*Ursus arctos*), Western population. https://species-registry.canada.ca/index-en.html#/species/1195-863

Stenhouse, G.B., J. Boulanger, M. Efford, S.B. Rovang, V.A. Sorensen and T. McKay. 2015. Estimates of grizzly bear population size and density for the 2014 Alberta Yellowhead Population Unit (BMA 3) and south Jasper National Park Inventory Project. Report prepared for Weyerhaeuser Ltd., West Fraser Mills Ltd, Alberta Environment and Parks, and Jasper National Park. https://friresearch.ca/sites/default/files/GBP_2015_10_Report_PopulationSize.pdf.

Tabachnick, B.G. and L.S. Fidell. 1996. Using multivariate statistics. Harper Collins, NY.

Underwood, A.J. 1997. Experiments in Ecology: Their Logical Design and Interpretation Using Analysis of Variance. Cambridge University Press, Cambridge.

Wickham, H. 2009. ggplot2: Elegant graphics for data analysis. Springer, NY.

Woods, J.G., D. Paetkau, D. Lewis, B.N. McLellan, M. Proctor and C. Strobeck. 1999. Genetic tagging free ranging black and brown bears. Wildlife Society Bulletin 27:616-627.

ACKNOWLEDGEMENTS

This study was funded by the Government of Northwest Territories. Kim Poole assisted with design, field implementation, and summaries of field methods for the first two years of this study. Stan Forsyth at Forsyth Lures graciously provided us with large quantities of very smelly liquids. The Department of Environment and Natural Resources Inuvik staff, notably Marsha Branigan, Steve Baryluk, Adam Thom, Christine Menno and Chris Laroque provided much appreciated assistance with the construction, deployment, sampling, and takedown of the hair-snag stations, and were good sports about getting splashed with rancid hog's blood in the process. Hunters and Trappers Committee members who assisted with fieldwork in 2019 included Randy Gruben from Tuktoyaktuk and Gerard Chicksi, William Day, and Max Kotokak Sr. from Inuvik. Helicopter support was provided by several pilots from Canadian Helicopters and Great Slave Helicopters in 2019, and by Connor Gould (Great Slave Helicopters) in 2020. David Paetkau and his team at Wildlife Genetics International were very helpful in the analysis of our samples.

APPENDIX 1

Background Information on Mark-recapture Issues

Several fundamental mark-recapture concepts must be defined to ensure adequate understanding of the concepts discussed in this report.

Definition of a Model and Estimator

Mark-recapture estimation represents an improvement from traditional count-based census methods. With traditional methods bears would be counted or trapped and the number trapped would be the estimate of population size. Inherent in this is the assumption that all animals have been trapped or counted, otherwise the estimate of population size would be lower than the actual population size. In mark-recapture estimation the percentage of animals captured is estimated. This percentage is called a capture probability. This concept can be expressed by the following formula:

$$\widehat{N} = \frac{\widehat{M}}{\hat{p}}$$

In the above formula, M is the count of animals, $\hat{p}$ is the estimate of capture probability, and $\widehat{N}$ is the estimate of population size. With traditional census methods $\hat{p}$ is assumed to equal one. An important term can be introduced here. A *model* is a set of assumptions that correspond to an estimation method. In the case of a census, our model is based on the assumption that all animals are caught. Capture probability $\hat{p}$ is rarely equal to one, and, as a result, many models have been formulated that make differing assumptions on how $\hat{p}$ varies. For any model there is a corresponding estimator. An *estimator* is a set of mathematical formulae that allow an estimate using the assumptions of the model. In the case of a count model, the estimate is simply the count of animals caught. The subject of estimation using mark-recapture methods has seen much theoretical attention and therefore, many estimators exist which are much more complex than simple counts.

Bias, Precision and Robustness

Estimates of density and population size are evaluated using two principal measures: precision and bias. The best way to conceptualize precision and bias is to consider what a range of estimates might look like if a project was repeated many times (Figure 22).

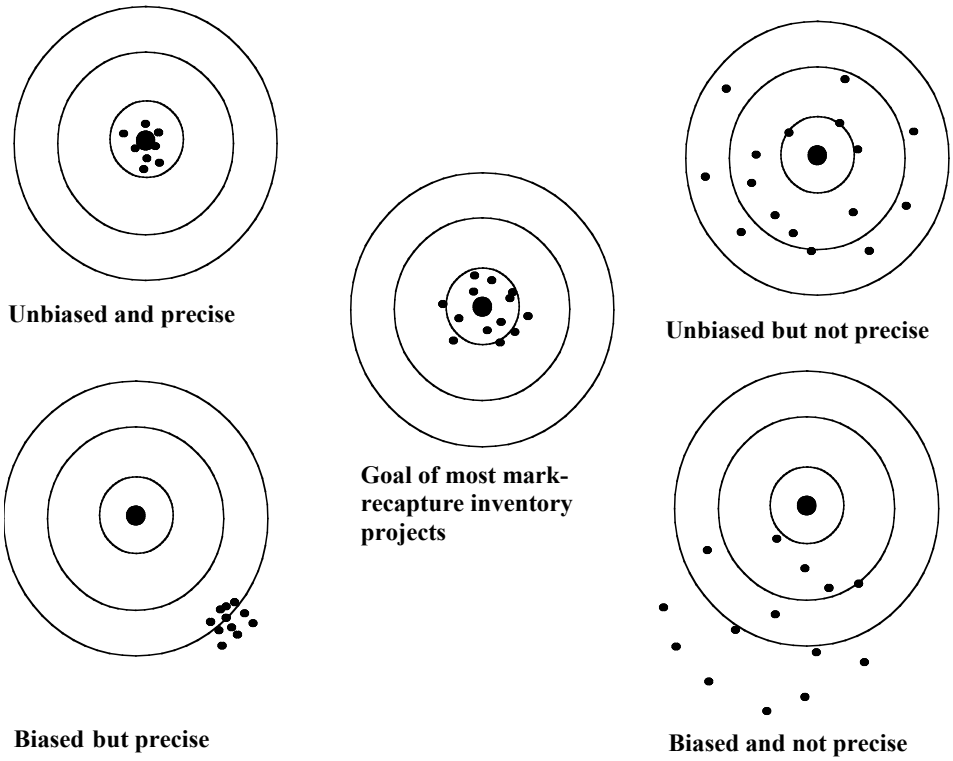

Figure 46. A conceptual diagram of bias and precision. Each target represents a possible set of estimates ("shots") from the mark-recapture experiment, if the study were repeated many times. Lack of precision is mainly caused by low sample sizes, and bias is caused by improper model selection. Unlike this target analogy, most mark-recapture experiments are only conducted once (i.e., one "shot") and the true bull's eye (true population size) is not known. Therefore, mark-recapture data should be interpreted cautiously and statistically to avoid erroneous conclusions.

Precision is the repeatability of estimates and is usually estimated by the coefficient of variation and the width of confidence intervals. *Bias* is the deviation of estimates from the true population value and is determined by how well the statistical model and estimator fit the mark-recapture data. The goal of most mark-recapture experiments is to minimize bias and maximize precision therefore minimizing potential error in estimates.

An ideal estimator of population size or density should be unbiased, precise, and robust. *Robustness* is a measure of how well an estimator will perform even when its associated assumptions about capture probability are violated. An example of a robust estimator would be one that assumes equal capture probabilities but still gives unbiased estimates when moderate capture probability variation exists in the data.

APPENDIX 2

Structural Relationships between Landcover Covariates

Principal components analysis was used to assess structural relationships among the primary habitat covariates. The principal components model explained 57% of the variation in the covariate data with the three principal components. Principal component scores suggested the higher association of shrub and lichen for the first component, closed spruce and deciduous (positive) and non-vegetated/sparse vegetated (negative) for the second loading and low shrub lowland and wet herbaceous for the third component (as determined by loads of greater than 0.5) (Table 18).

Table 38. Standardized component scores for principal components analysis of SECR habitat mask remote sensing data. Significant factors are in bold.

Variable	Factor1	Factor2	Factor3
Closed spruce	0.17	**0.61**	-0.33
Deciduous	0.07	**0.59**	-0.48
Dwarf shrub	**-0.84**	0.14	-0.02
Low shrub lowland	0.47	-0.09	**0.67**
Low shrub upland	**-0.83**	-0.13	0.20
Open spruce	0.32	0.35	-0.06
Tall shrub	0.48	0.38	0.18
Tussock lichen	**-0.71**	-0.18	0.31
Water	0.24	-0.27	-0.18
Wet herbaceous	0.47	0.35	**0.56**
Herbaceous	0.40	-0.45	0.23
Non-vegetated	0.41	**-0.65**	-0.30
Sparse vegetation	0.27	**-0.62**	-0.39

Inspection of principal component plots suggested positive associations of higher elevation communities (dwarf shrub, low shrub upland, tussock lichen) for the first component (Figure 23). The second component was positively associated by closed canopy vegetation (closed spruce/deciduous/closed birch) but negatively associated with sparse/non-vegetation areas. The third component was less associated with any particular class. These results suggest that the dominant gradients are towards association of higher elevation communities (first component) and closed cover in opposition to sparse/non vegetated classes in the second component. The main interpretation of this result is that association of any particular habitat class may indicate a general gradient in the data set as opposed to a single association (as discussed later).

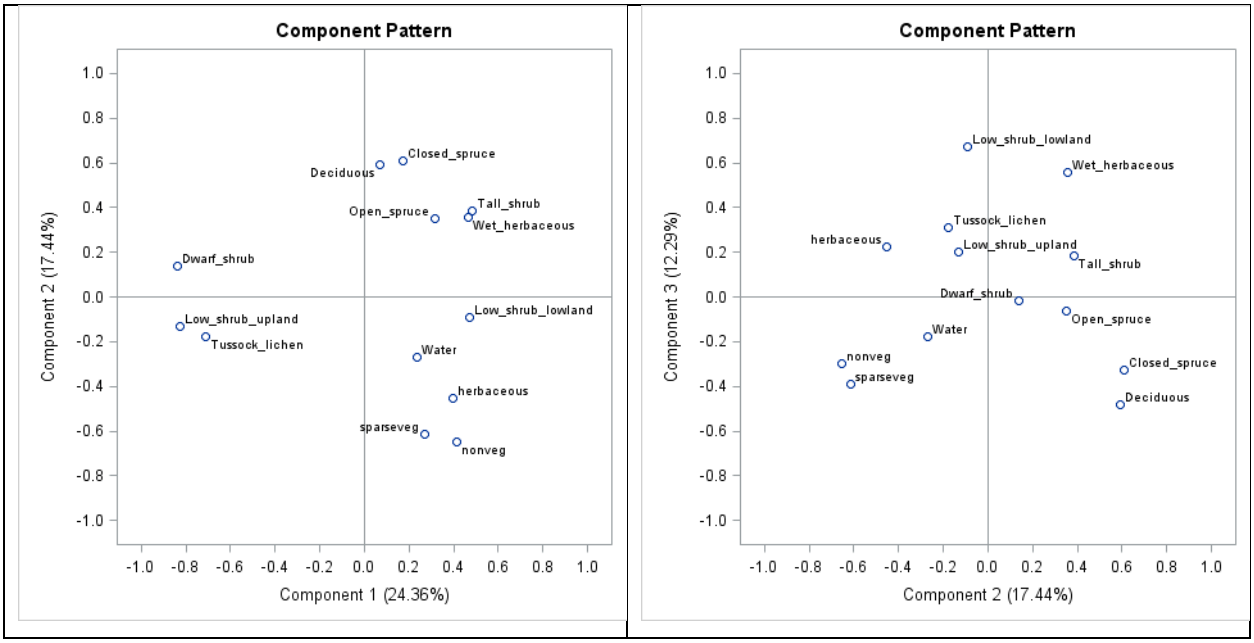

Figure 47. Plots of principal component scores (Table 8) for mask centroid covariates.

APPENDIX 3

Details on Mortality Surfaces

Below are plots depicting the mortality surfaces used in density surface modeling (Figure 24). The basic approach of the analysis was to tally mortality locations each year and assign buffers for males and females based on home range areas. The number of buffers intersecting each mask point was then tallied and scaled across the mask to create a mortality level covariate (for immediate yearly mortality, mortalities that occurred in the past three year and ten years).

Current year

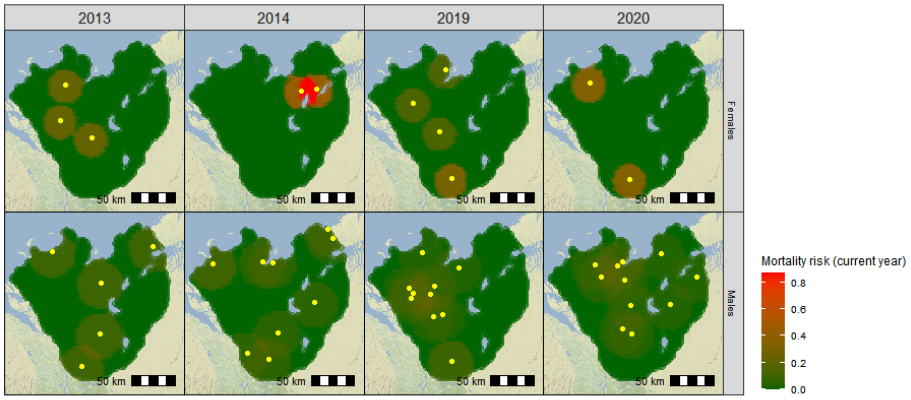

Last 3 years

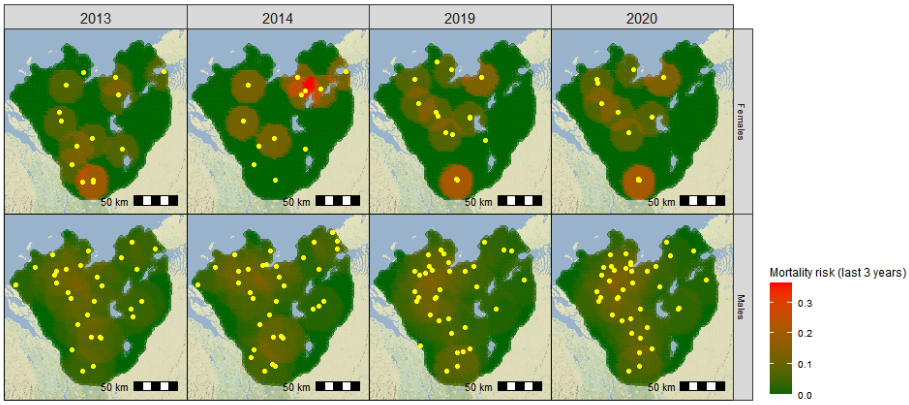

Last 10 years

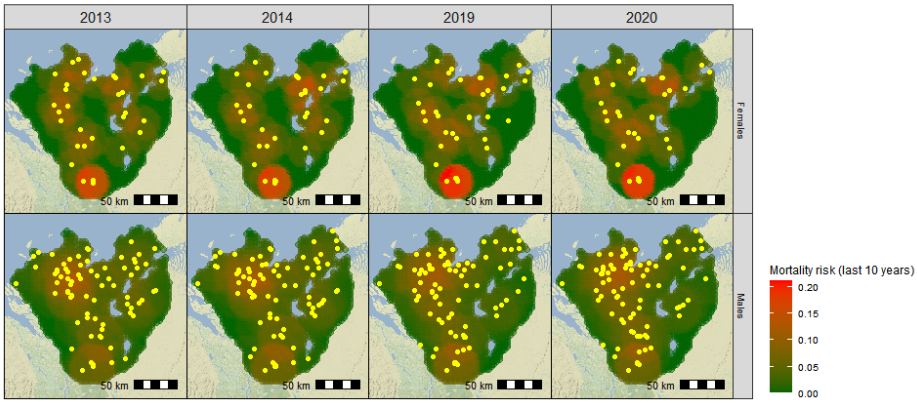

Figure 48. Examples of mortality risk mask covariates for males and females. Mortality locations are shown in yellow.

APPENDIX 4

Full Listings of Density Surface Model Selection

Table 39. Female spatially explicit density surface modeling model selection results. A base model (g_0 (bk), sigma (.)) was used for all analyses except when noted. An exponential relationship between covariates and density was assumed except where noted. The base model (with no density covariates) is shaded in grey. Sample size adjusted AIC_c, the difference in AIC_c between the most supported model for each model (ΔAIC_c), AIC_c weight (w_i), number of model parameters (K) and log-likelihood (LL) are given.

No	Landcover	Road/Temporal	Mortality	AIC_c	$dAIC_c$	w_i	K	LL
1	decid + shrub + herb	spline(df=3)		2471.3	0.00	0.36	9	-1226.2
2	decid + shrub + herb	spline(df=3)	FpMortsYr	2473.1	1.73	0.15	10	-1225.9
3	decid + shrub + herb	Period+spline(df=3)		2473.5	2.20	0.12	10	-1226.1
4	decid + shrub + herb	ZOIHR		2474.0	2.62	0.10	8	-1228.6
5	decid + shrub + herb	ZOIsig		2475.1	3.80	0.05	8	-1229.2
6	decid + shrub + herb	StrataHR		2475.2	3.87	0.05	8	-1229.2
7	decid + shrub + herb	spline(df=3)+Period	FpMortsYr	2475.3	3.98	0.05	11	-1225.9
8	decid + shrub + herb	Period*ZOIHR		2476.1	4.78	0.03	9	-1228.5
9	decid + shrub + herb	Period+ZOIHR		2476.1	4.80	0.03	9	-1228.6
10	decid + shrub + herb	Period*ZOIsig		2477.3	5.97	0.02	9	-1229.1
11	decid + shrub + herb	Period+ZOIsig		2477.3	5.97	0.02	9	-1229.1
12	decid + shrub + herb	Period*spline(df=3)		2479.2	7.90	0.01	13	-1225.6
13	decid + shrub + herb	Period*Strata		2481.8	10.45	0.00	11	-1229.1
14	decid + shrub + herb	spline(Post-road,df=3)		2485.5	14.19	0.00	9	-1233.3
15	decid + shrub + herb			2485.9	14.53	0.00	7	-1235.6
16	decid + shrub + herb	spline(Pre-road,df=3)		2487.2	15.90	0.00	9	-1234.1
17	decid + shrub + herb		FpMortsYr	2487.4	16.10	0.00	8	-1235.3
18	decid + shrub + herb		FpMorts10	2487.7	16.41	0.00	8	-1235.5
19	decid + shrub + herb		FpMortsLag2	2487.8	16.48	0.00	8	-1235.5
20	decid + shrub + herb	Period		2488.0	16.67	0.00	8	-1235.6
21	decid + herb			2495.4	24.10	0.00	6	-1241.5
22	decid			2497.0	25.69	0.00	5	-1243.4
24	forestF			2512.2	40.88	0.00	5	-1250.9
25	waterF			2536.8	65.47	0.00	5	-1263.2
26	shrub			2547.8	76.42	0.00	5	-1268.7
27	elevation			2554.1	82.80	0.00	5	-1271.9
28	TRI			2554.5	83.17	0.00	5	-1272.1

No	Landcover	Road/Temporal	Mortality	AIC_c	$dAIC_c$	w_i	K	LL
29	herb			2564.4	93.07	0.00	5	-1277
30	barren			2565.3	93.99	0.00	5	-1277.5
31	Period			2585.4	114.03	0.00	5	-1287.5
32	constant			2587.4	116.03	0.00	6	-1287.4
33	year			2589.2	117.82	0.00	7	-1287.3

Table 40. Male spatially explicit density surface modeling model selection results. A base model (g_0 (B), sigma (.)) was used for all analyses except when noted. An exponential relationship between covariates and density was assumed except where noted. The base model (with no density covariates) is shaded in grey. Sample size adjusted AIC_c, the difference in AIC_c between the most supported model for each model (ΔAIC_c), AIC_c weight (w_i), number of model parameters (K) and log-likelihood (LL) are given.

No	LC	Road	Mortality	AIC_c	$dAIC_c$	w_i	K	LL
1	decid	ZOIHR*period		1,609.37	0.00	0.18	7	-797.1
2	decid	ZOIHR+periods		1,609.86	0.48	0.14	7	-797.4
3	decid	ZOIHRpre		1,610.13	0.75	0.12	6	-798.6
4	decid	ZOIHR*period	MortsLag2	1,610.82	1.45	0.09	8	-796.7
5	decid	ZOIHR*period	MortsLag10	1,610.97	1.60	0.08	8	-796.7
6	decid	ZOIHR*period	MortsYr	1,611.09	1.71	0.08	8	-796.8
7	decid	spline(Road,df=4)		1,611.46	2.09	0.06	8	-797.0
8	decid	ZOIHR		1,612.59	3.22	0.04	6	-799.9
9	decid	spline(Road,df=4)		1,612.79	3.41	0.03	8	-797.7
10	decid	spline(Road,df=4)*Period		1,613.01	3.63	0.03	11	-794.1
11	decid	Period		1,613.04	3.66	0.03	6	-800.1
12	decid	spline(Roadpre)		1,613.43	4.06	0.02	8	-798.0
13	decid	ZOIHR*year		1,614.07	4.70	0.02	9	-797.1
14	decid	ZOIpost		1,614.35	4.98	0.01	6	-800.8
15	decid	spline(Road,df=3)*Period		1,614.80	5.42	0.01	9	-797.5
16	decid	ZOIsig		1,615.25	5.88	0.01	7	-800.1
17	decid	spline(Road,df=3)		1,615.81	6.44	0.01	7	-800.3
18	decid+shrub			1,615.87	6.50	0.01	6	-801.5
19	decid			1,616.13	6.76	0.01	5	-802.8
20	decid+herb+shrub			1,616.86	7.48	0.00	7	-800.9
21	decid		MortsLag2	1,617.37	7.99	0.00	6	-802.3
22	decid		MortsYr	1,617.38	8.01	0.00	6	-802.3
23	decid	StrataHR*Period		1,617.51	8.13	0.00	9	-798.8
24	decid	Year		1,617.58	8.21	0.00	8	-800.0
25	decid	ZOIsig*Period		1,617.93	8.55	0.00	7	-801.4
26	decid		MortsLag10	1,617.97	8.60	0.00	6	-802.6
27	decid	Spline(Roadpost)		1,617.99	8.61	0.00	8	-800.3
28	forest			1,628.49	19.12	0.00	5	-808.9

No	LC	Road	Mortality	AIC_c	$dAIC_c$	w_i	K	LL
29	water			1,637.14	27.77	0.00	5	-813.3
30	elevation			1,637.23	27.86	0.00	5	-813.3
31	shrub			1,637.91	28.54	0.00	5	-813.7
32	herb			1,638.25	28.87	0.00	5	-813.8
33	TRI			1,641.30	31.92	0.00	5	-815.3
34	RSF			1,647.91	38.54	0.00	5	-818.7
35	constant			1,648.27	38.90	0.00	4	-819.9
36	Year			1,649.62	40.25	0.00	7	-817.2